

A COMPLETE 3-DIMENSIONAL BLASCHKE-SANTALÓ DIAGRAM

RENÉ BRANDENBERG AND BERNARDO GONZÁLEZ MERINO

ABSTRACT. We present a complete 3-dimensional Blaschke-Santaló diagram for planar convex bodies with respect to the four classical magnitudes inner and outer radius, diameter and (minimal) width in euclidean spaces.

1. INTRODUCTION

The focus of the paper are the standard radii measured for the family \mathcal{K}^n of convex bodies $K \subset \mathbb{R}^n$, where a convex body is a compact and convex set in euclidean n -space. The *diameter* $D(K)$ of K is the biggest distance between two points of K , the *width* $w(K)$ is the minimal *breadth*, i. e. the smallest distance between any two different parallel supporting hyperplanes of K . The *inradius* $r(K)$ is the radius of a biggest ball contained in K , and the *circumradius* $R(K)$ is the radius of the (unique) smallest ball containing K .

A natural and very intuitive question is the following: if $K \in \mathcal{K}^n$ is given and we have fixed values for some of the previous radii (say e. g. r , D and R), which is the range of possible values of w depending on r , D and R ? A comprehensive solution of this task in \mathcal{K}^2 is presented in the following in form of a Blaschke-Santaló diagram (sometimes also called shape diagram).

Let us start with some historical and more general review: In [1] Blaschke proposed the study of possible values for the volume $V(K)$, surface area $S(K)$, and integral mean curvature $M(K)$ for any $K \in \mathcal{K}^3$. For doing so, he considered the mapping

$$h : \mathcal{K}^3 \rightarrow [0, 1]^2, \text{ with } h(K) := \left(\frac{4\pi S(K)}{M(K)^2}, \frac{48\pi^2 V(K)}{M(K)^3} \right).$$

The image $h(\mathcal{K}^3)$ is well known as *Blaschke diagram*. Blaschke realized that the isoperimetric inequality and the geometric inequalities of Minkowski were not sufficient for a complete description of $h(\mathcal{K}^3)$. A *complete system of inequalities* needed additional geometric inequalities relating V , S and M , still a famous open problem in convex geometry, see [12, 16].

Reviving the idea of Blaschke, Santaló proposed in [17] the study of such diagrams for all triples of the magnitudes r , w , D , R , p (perimeter) and A (area), for a start, for planar sets. Once a triple is fixed, say (r, D, R) , the function

$$g : \mathcal{K}^2 \rightarrow [0, 1]^2, \text{ with } g(K) := \left(\frac{r(K)}{R(K)}, \frac{D(K)}{2R(K)} \right)$$

is considered, and its image $g(\mathcal{K}^2)$ is called a *Blaschke-Santaló diagram*. Full descriptions of those diagrams for the triples (A, p, w) , (A, p, r) , (A, p, R) , (A, w, D) , (p, w, D) , and (r, D, R) are already derived in [17].

2000 *Mathematics Subject Classification*. Primary 52A10, 52A40; Secondary 52A20.

Key words and phrases. Inner and outer radii, geometric inequalities, Blaschke diagram, Blaschke-Santaló diagram, shape diagrams.

The second author was partially supported by MINECO (Ministerio de Economía y Competitividad) and FEDER (Fondo Europeo de Desarrollo Regional) project MTM2012-34037, and La Fundación Séneca Región de Murcia, under the programme *Becas-contrato predoctorales de formación del personal investigador*, 2008.

An important first ingredient in the full description of the diagram for (r, D, R) in [17] are the well known (and easy to prove) inequalities

$$(1) \quad 2r(K) \leq w(K) \leq D(K) \leq 2R(K)$$

as well as the inequality of Jung [14]

$$(2) \quad R(K) \leq \sqrt{\frac{n}{2(n+1)}} D(K)$$

which are true for all $K \in \mathcal{K}^n$.

Moreover the validity of the inequalities

$$(3) \quad w(K) \leq r(K) + R(K) \leq D(K)$$

was shown in [17] (there only for $n = 2$, but easy to see to be true in general dimensions, see e.g. [4]). Equality in (3) holds true simultaneously, if K is of constant width (i.e. if $w(K) = D(K)$). See [6] for more details and extensions on (3).

A final inequality derived in [17] holds true (in the given form) for $K \in \mathcal{K}^2$ only:

$$2R(K) \left(2R(K) + \sqrt{4R(K)^2 - D(K)^2} \right) r(K) \geq D(K)^2 \sqrt{4R(K)^2 - D(K)^2},$$

with equality, if K is an isosceles triangle.

This inequality, together with Jung's inequality (2) and the relevant parts of (1) and (3) forms a complete system of inequalities for (r, D, R) .

Moreover, Santaló observed that previously known inequalities did not form complete systems of inequalities in any case of changing one of (r, D, R) to the width w .

In [10] and [13] Hernández Cifre and Segura Gomis could state the missing inequalities:

$$(4) \quad \begin{aligned} (4R(K)^2 - D(K)^2)D(K)^4 &\leq 4w(K)^2R(K)^4, \\ (4r(K) - w(K))(w(K) - 2r(K))R(K) &\leq 2r(K)^3, \\ D(K)^4(w(K) - 2r(K))^2(4r(K) - w(K)) &\leq 4r(K)^4w(K), \text{ and} \\ \sqrt{3}(w(K) - r(K)) &\leq D(K). \end{aligned}$$

Moreover, they showed that those of the new inequalities together with those in (1) to (3), which do only involve the appropriate radii, form complete systems of inequalities for the triples (w, D, R) , (r, w, R) and (r, w, D) . In [11] Hernández Cifre computed complete systems of inequalities for the triples (A, D, R) and (p, D, R) and Böröczky Jr., Hernández Cifre, and Salinas gave complete diagrams for the triples (A, r, R) and (p, r, R) in [3].

Thus all 4 Blaschke-Santaló diagrams of \mathcal{K}^2 involving only the classical radii r, w, D , and R could be completed, but there are still 7 out of the 20 possible triples involving also A and p where a full description of the diagram is still missing or at least unproven.

Recently, Blaschke-Santaló diagrams have been used in pattern recognition and image analysis (see [7, 8, 15]), as they help in the prediction of the size and shape of 3-dimensional sets from their 2-dimensional projections. In [7, 15] for example, the diagrams (in this context mostly called shape-diagrams) have been combined with probabilistic methods, such as maximum likelihood estimation in the second of them.

Once there are complete systems of inequalities for some of the possible triples of magnitudes amongst A, p, r, w, D, R , it is a natural step to consider complete systems of inequalities for even more than three of those magnitudes, e.g. to obtain stronger inequalities or for an even more accurate classification of convex sets in the mentioned application in image analysis. In [21] the quadruple (A, p, w, D) has been considered, without deriving a complete description (which is not so much surprising, as even for the triple (A, p, D) a complete description is still missing). We consider the case (r, w, D, R) , which is the unique diagram involving four

of the above magnitudes, s. t. for all choices of triples of them complete descriptions of the diagrams are known. To the best of our knowledge, besides [21] and the preliminary work of this paper in [4], it is the only paper considering more than three of these magnitudes.

The study shows the necessity of *new inequalities* relating all four radii at once. This is done by describing the diagram's skeleton, i. e. its boundary structure consisting of 0-, 1-, and 2-dimensional differential manifolds (see below for a proper definition).

Further notation is the following: If $l \in \mathbb{N}$, we abbreviate $[l] := \{1, \dots, l\}$. For a general set $C \subset \mathbb{R}^n$, we write $\text{aff}(C)$ and $\text{conv}(C)$ for the *affine hull* and the *convex hull* of C , respectively, and for any $x, y \in \mathbb{R}^n$ we denote by $[x, y]$ the *segment* $\text{conv}\{x, y\}$ whose endpoints are x and y . If $K \in \mathcal{K}^n$ we write $\text{ext}(K)$ for the set of *extreme points* of K and any $x \in \text{ext}(K)$ is said to be *exposed*, if there exists a hyperplane H supporting K , s. t. $K \cap H = \{x\}$.

The euclidean unit ball and unit sphere are denoted by $\mathbb{B}, \mathbb{S} \subset \mathbb{R}^n$, respectively, and the closed (open) *semisphere* $\{x \in \mathbb{S} : u^T x \geq 0\}$ ($\{x \in \mathbb{S} : u^T x > 0\}$) with $u \in \mathbb{R}^n \setminus \{0\}$, by \mathbb{S}_u^\geq ($\mathbb{S}_u^>$). By $\text{dist}(A, B)$ we denote the usual euclidean distance between two closed sets $A, B \subset \mathbb{R}^n$, and write $\text{dist}(a, B)$ or $\text{dist}(A, b)$ if one of the sets is a singleton.

For a pair of bodies $K, L \in \mathcal{K}^n$, the *Minkowski sum* of K and L is defined as

$$K + L := \{x_1 + x_2 : x_1 \in K, x_2 \in L\},$$

and $\lambda K := \{\lambda x : x \in K\}$ with $\lambda \in \mathbb{R}$ is the λ *dilatation* of K . We abbreviate $K - L := K + (-L)$ and $K + x := K + \{x\}$ for $x \in \mathbb{R}^n$. A body K is *0-symmetric* if $K = -K$ and *centrally symmetric* if there exists $c \in \mathbb{R}^n$, s. t. $K - c$ is 0-symmetric.

For any body $K \in \mathcal{K}^n$, a *completion* of K is defined as a set C_K satisfying $K \subset C_K$ and $D(K) = D(C_K) = w(C_K)$. Moreover, C_K is called a *Scott-completion* of K if, in addition, $R(K) = R(C_K)$ (it was shown in [19] that in euclidean space such a completion always exists).

We go on with a little series of well known propositions, which we will use later. The first collects results taken from [9]:

Proposition 1.1. *For any $K \in \mathcal{K}^n$*

- a) *every diametral pair of points in K is a pair of exposed (and therefore extreme) points in K .*
- b) *every pair L_1, L_2 of parallel supporting hyperplanes of K at distance $w(K)$, supports a segment with endpoints in $K \cap L_1$ and $K \cap L_2$ perpendicular to both hyperplanes. Moreover, if $K \in \mathcal{K}^n$ is a polyhedron, then $\dim(K \cap L_1) + \dim(K \cap L_2) \geq d - 1$ (which in case of $n = 2$ means that at least one of the intersections $K \cap L_i$, $i = 1, 2$ contains a segment).*

The first part of the following proposition about the euclidean outer radius was shown already in [2]. For the part about the inner radius we refer to the general optimality conditions for containment under homothetics given in [5].

Proposition 1.2. *Let $K \in \mathcal{K}^n$ and $c \in \mathbb{R}^n$, s. t. $c + \rho \mathbb{B} \subset K \subset \mathbb{B}$. Then*

- a) *$R(K) = 1$, iff there exist $k \in \{2, \dots, n + 1\}$ and $p^1, \dots, p^k \in \text{bd}(K \cap \mathbb{S})$ s. t. $0 \in \text{conv}\{p^1, \dots, p^k\}$.*
- b) *$r(K) = \rho$, iff there exists $l \in \{2, \dots, n + 1\}$, $q^1, \dots, q^l \in \text{bd}(K - c) \cap \rho \mathbb{S}$ and $u^1, \dots, u^l \in \mathbb{S}$, s. t. $(u^i)^T q^i = \rho$, $i \in [l]$, $K - c \subset \bigcap_{i \in [l]} \{x \in \mathbb{R}^n : (u^i)^T x \leq \rho\}$, and $0 \in \text{conv}\{u^1, \dots, u^l\}$.*

The last proposition is ancient and best known as the “inscribed angle theorem”:

Proposition 1.3. *For any triangle $T := \text{conv}\{p^1, p^2, p^3\}$ with $p^1, p^2, p^3 \in \mathbb{S}$ and 0 and p^3 on the same side of $\text{aff}\{p^1, p^2\}$ let γ denote the angle of T at p^3 . Then the angle of the triangle $\text{conv}\{p^1, p^2, 0\}$ at 0 is 2γ (independently of the position of p^3).*

Moreover, if $p^3 \in \text{int}(\mathbb{B})$ (or $p^3 \notin \mathbb{B}$), but still on the same side of $\text{aff}\{p^1, p^2\}$ than 0 , the angle in 0 is strictly smaller (or, respectively, strictly greater) than 2γ .

In Section 2 the way we proceed for the description of the whole diagram is explained.

In Section 3 we present a collection of nine (generally) valid inequalities completely describing the diagram in Section 2. Six of these inequalities were known before but three of them are totally new, relating all four basic radii at once (in a non-trivial way).

Every family of sets attaining equality in one of the inequalities above is mapped onto a compact connected subset of a 2-dimensional differential manifold within \mathbb{R}^3 . We call them *facets* of the diagram. Moreover, the common boundaries between any two facets are called *edges* of the diagram and the bodies appearing in the intersection of three (or more) facets are called *vertices* of the diagram. The families forming the facets and edges, as well as all vertices are described in Section 4.

Section 5 is devoted to the proofs of the new inequalities presented in Section 3, while the paper is finished with a short outview in Section 6.

2. MAIN IDEAS FOR EXPLAINING THE DIAGRAM

Following the idea of Blaschke and Santaló, we define

$$(5) \quad f : \mathcal{K}^n \rightarrow [0, 1]^3, \quad f(K) = \left(\frac{r(K)}{R(K)}, \frac{w(K)}{2R(K)}, \frac{D(K)}{2R(K)} \right)$$

and call $f(\mathcal{K}^n)$ a *3-dimensional Blaschke-Santaló diagram*. The following Lemma is taken from [4]:

Lemma 2.1. $f(\mathcal{K}^n) = f(\{K \in \mathcal{K}^n : \mathbb{B} \text{ is the circumball of } K\})$ is starshaped with respect to $f(\mathbb{B}) = (1, 1, 1)$.

Proof. If $K \in \mathcal{K}^n$, $c \in \mathbb{R}^n$, $\lambda \in [0, 1]$ and q any of the four radii functionals r, w, D, R , it obviously holds $q(\lambda(K + c)) = \lambda q(K)$ and $q(\lambda K + (1 - \lambda)\mathbb{B}) = \lambda q(K) + (1 - \lambda)q(\mathbb{B})$. \square

The latter part of Lemma 2.1 means that the diagram has no “holes” and therefore it suffices to describe the sets $K \in \text{bd}(\mathcal{K}^n)$, with \mathbb{B} being their circumball, mapped to the boundary of the diagram.

Lemma 2.2. Let $K, C_K \in \mathcal{K}^n$, s. t. C_K is a completion of K and $K_\lambda := \lambda K + (1 - \lambda)C_K$, $\lambda \in [0, 1]$. Then $D(K_\lambda) = D(K)$ and $w(K_\lambda) = \lambda w(K) + (1 - \lambda)w(C_K)$ for all $\lambda \in [0, 1]$.

Proof. Since $K \subset C_K$ and $D(K) = D(C_K)$ it immediately follows from $K \subset K_\lambda \subset C_K$ that $D(K_\lambda) = D(K)$ for every $\lambda \in [0, 1]$. Now, let $s^* \in \mathbb{S}$, s. t. the breadth $b_{s^*}(K)$ of K in direction of s^* is $b_{s^*}(K) = w(K)$. Since C_K is of constant width and because the breadth is linear with respect to the Minkowski sum, we obtain

$$\begin{aligned} w(K_\lambda) &= \min_{s \in \mathbb{S}} b_s(K_\lambda) = \min_{s \in \mathbb{S}} (\lambda b_s(K) + (1 - \lambda)w_s(C_K)) \\ &\leq \lambda b_{s^*}(K) + (1 - \lambda)w(C_K) = \lambda w(K) + (1 - \lambda)w(C_K) \leq w(K_\lambda). \end{aligned}$$

\square

Lemma 2.3. For any $K \in \mathcal{K}^n$ satisfying the left inequality in (3) with equality (i. e. $w(K) = r(K) + R(K)$), C_K being its Scott-completion, and $K_\lambda := \lambda K + (1 - \lambda)C_K$, $\lambda \in [0, 1]$, it holds $f(K_\lambda) = \lambda f(K) + (1 - \lambda)f(C_K)$ and therefore $w(K_\lambda) = r(K_\lambda) + R(K_\lambda)$ for all $\lambda \in [0, 1]$.

Proof. Using Lemma 2.2 it immediately follows that $D(K_\lambda) = D(K)$, $R(K_\lambda) = R(K)$, and $w(K_\lambda) = \lambda w(K) + (1 - \lambda)w(C_K)$ for all $\lambda \in [0, 1]$.

In [4] it was shown that $w(K) = r(K) + R(K)$ implies that K has a unique inball being concentric with the circumball.

Hence, assuming as always that \mathbb{B} is the circumball of K , we have $r(K)\mathbb{B} \subset K \subset \mathbb{B}$ with $R(K) = 1$.

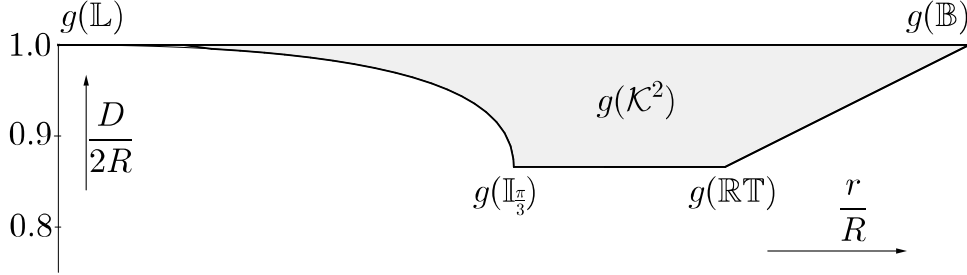


FIGURE 1. The diagram $g(\mathcal{K}^2)$ with x -axis r/R and y -axis $D/2R$. The boundaries are given via the inequalities collected in (6). The vertices are the euclidean ball \mathbb{B} , the line segment \mathbb{L} , the equilateral triangle $\mathbb{I}_{\pi/3}$ and the Reuleaux triangle \mathbb{RT} (see Subsection 4.1 for their explanation).

Observe that if $s \in \mathbb{S}$ with $-r(K)us \in \text{bd}(K)$, then $s \in K$. This follows because the (unique) supporting hyperplane in $-r(K)s$ of K has to support $r(K)\mathbb{B}$ too, and therefore this hyperplane has to be $-r(K)s + \text{lin}\{s\}^\perp$. Thus the breadth of K in the direction s is at most $r(K) + R(K)$, with equality iff $s \in K$.

Using Proposition 1.2 there exist $u^1, \dots, u^j \in \mathbb{S}$, $2 \leq j \leq n+1$, s. t. $-r(K)u^i \in \text{bd}(K)$, $i \in [j]$ with $0 \in \text{conv}\{u^1, \dots, u^j\}$, which together with the observation above yields that $u^i \in K \cap \mathbb{S}$ and that the hyperplanes $-r(K)u^i + \text{lin}\{u^i\}^\perp$ support K in $-r(K)u^i$, $i \in [j]$.

Now, since C_K is a Scott-completion of K it obviously holds $r(C_K)\mathbb{B} \subset C_K \subset \mathbb{B}$, $u^i \in C_K$, and since $w(C_K) = r(C_K) + R(C_K)$ also that the hyperplanes $-r(C_K)u^i + \text{lin}\{u^i\}^\perp$ support C_K and its inball in $-r(C_K)u^i$, $i \in [j]$.

Altogether we obtain $-r(K)u^i + \text{lin}\{u^i\}^\perp$ and $-r(C_K)u^i + \text{lin}\{u^i\}^\perp$ support K and C_K in the points $-r(K)u^i$ and $-r(C_K)u^i$, respectively. Hence the hyperplanes $-(\lambda r(K) + (1-\lambda)r(C_K))u^i + \text{lin}\{u^i\}^\perp$ support $\lambda K + (1-\lambda)C_K$ in the points $-(\lambda r(K) + (1-\lambda)r(C_K))u^i$, $i \in [j]$. Using again Proposition 1.2, it follows $r(\lambda K + (1-\lambda)C_K) = \lambda r(K) + (1-\lambda)r(C_K)$ and from this the rest of the statement in the lemma. \square

As mentioned in Section 1 the inequalities

$$(6) \quad \begin{aligned} D(K) &\leq 2R(K), \quad D(K) \geq r(K) + R(K), \quad D(K) \geq \sqrt{3}R(K), \quad \text{and} \\ 2R(K) \left(2R(K) + \sqrt{4R(K)^2 - D(K)^2} \right) r(K) &\geq D(K)^2 \sqrt{4R(K)^2 - D(K)^2}, \end{aligned}$$

give a full description of

$$g : \mathcal{K}^2 \rightarrow [0, 1]^2, \quad \text{with } g(K) := \left(\frac{r(K)}{R(K)}, \frac{D(K)}{2R(K)} \right)$$

(see Figure 1).

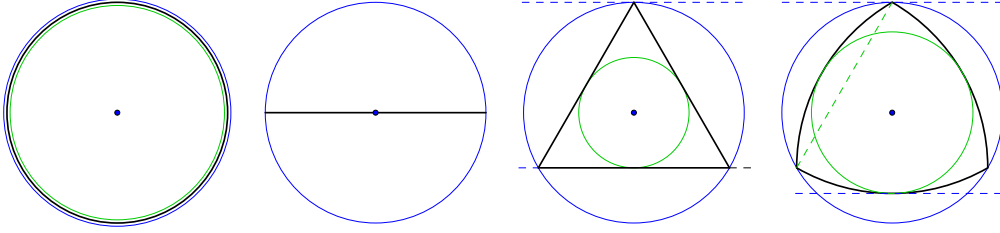


FIGURE 2. From left to right: the euclidean ball \mathbb{B} , the line \mathbb{L} , the equilateral triangle $\mathbb{I}_{\pi/3}$, and the Reuleaux triangle \mathbb{RT} . Here and in all the forthcoming figures, the inballs are drawn in green, the circumballs in blue, the diameters in dashed green, and the widths in dashed blue.

Since $g(\mathcal{K}^2)$ is just the projection of $f(\mathcal{K}^2)$ onto the first and last coordinate, we may consider any valid pair of values $(r, D) \in g(\mathcal{K}^2)$ and solve

$$\begin{array}{l} \max_{K \in \mathcal{K}^2} w(K) \\ r(K) = r \\ D(K) = D \\ R(K) = 1 \end{array} \quad \text{as well as} \quad \begin{array}{l} \min_{K \in \mathcal{K}^2} w(K) \\ r(K) = r \\ D(K) = D \\ R(K) = 1 . \end{array}$$

Calling the solution of the maximization problem $w^*(r, D)$ for any given pair (r, D) and the solution of the minimization problem $w_*(r, D)$, the family $\{w^*(r, D) : (r, D) \in g(\mathcal{K}^2)\}$ describes the upper boundary of $f(\mathcal{K}^2)$ and $\{w_*(r, D) : (r, D) \in g(\mathcal{K}^2)\}$ describes the lower boundary of $f(\mathcal{K}^2)$. To complete the full diagram it then suffices to check which of the inequalities in (6) still describe facets of $f(\mathcal{K}^2)$ (i. e. there exists a pair $(r, D) \in \text{bd}(g(\mathcal{K}^2))$, s. t. the corresponding inequality is fulfilled with equality and $w^*(r, D) \neq w_*(r, D)$) and which describe only edges (which is the case if $w^*(r, D) = w_*(r, D)$ for all $(r, D) \in g(\mathcal{K}^2)$ fulfilling the inequality with equality).

3. MAIN INEQUALITIES

In this section we describe nine valid inequalities. Three of them are of the form $w \leq w^*(r, D)$, thus describing the upper boundary of the diagram; we call them (ub_j) , $j = 1, 2, 3$. Analogously, we write (lb_j) , $j = 1, 2, 3$ for the three inequalities $w \geq w_*(r, D)$ (giving the lower boundary) and (ib_j) , $j = 1, 2, 3$ for the inequalities which are independent of w .

We start with those inequalities which are a-priori known:

Proposition 3.1. *Let $K \in \mathcal{K}^2$. Then*

$$\begin{array}{ll} (lb_1) & 2r(K) \leq w(K) \\ (ib_1) & D(K) \leq 2R(K) \\ (ub_1) & w(K) \leq R(K) + r(K) \\ (ib_2) & R(K) + r(K) \leq D(K) \\ (ib_3) & \sqrt{3}R(K) \leq D(K) \\ (lb_2) & (4R(K)^2 - D(K)^2)D(K)^4 \leq 4w(K)^2R(K)^4 \end{array}$$

The remaining three inequalities for a complete description of $f(\mathcal{K}^2)$ are new. Surely, each of them involves all four radii r, w, D , and R simultaneously as otherwise it would have been necessary for the description of the according 2-dimensional Blaschke-Santaló diagram.

Theorem 3.2. *Let $K \in \mathcal{K}^2$. Then*

(lb₃)

$$w(K) \geq 2D(K) \sqrt{1 - \left(\frac{D(K)}{2R(K)}\right)^2} \cos \left[\arccos \left(\frac{D(K)}{2(D(K) - r(K))} \right) + \arccos \left(\frac{D(K)}{2R(K)} \right) - \arcsin \left(\frac{r(K)}{D(K) - r(K)} \right) \right]$$

Remark 3.3. *An algebraic representation of (lb₃) can easily be calculated using a computer algebra tool and looks like the following:*

$$w(K) \geq 2D(K) \sqrt{1 - \left(\frac{D(K)}{2R(K)}\right)^2} \left[\sqrt{1 - \frac{r(K)^2}{(D(K) - r(K))^2}} \left(\frac{D(K)^2}{4R(K)(D(K) - r(K))} - \sqrt{\left(1 - \frac{D(K)^2}{4(D(K) - r(K))^2}\right) \left(1 - \frac{D(K)^2}{4R(K)^2}\right)} \right) + \frac{r(K)}{D(K) - r(K)} \left(\frac{D(K)}{2R(K)} \sqrt{1 - \frac{D(K)^2}{4(D(K) - r(K))^2}} - \frac{D(K)}{2(D(K) - r(K))} \sqrt{1 - \frac{D(K)^2}{4R(K)^2}} \right) \right]$$

Theorem 3.4. *Let $K \in \mathcal{K}^2$. Then*

$$(ub_2) \quad w(K) \leq r(K) \left(1 + \frac{2\sqrt{2}R(K)}{D(K)} \sqrt{1 + \sqrt{1 - \left(\frac{D(K)}{2R(K)}\right)^2}} \right).$$

Remark 3.5. *One may recognize that*

$$1 + \frac{(2\sqrt{2}R(K))}{D(K)} \sqrt{1 + \sqrt{1 - \left(\frac{D(K)}{2R(K)}\right)^2}} \leq 3,$$

which shows that (ub₂) is a direct strengthening of the 2-dimensional version of Steinhagen's inequality (cf. [20]). However, this is not the case for (ub₃) (even so containing \mathbb{L} and $\mathbb{I}_{\pi/3}$, the two sets fulfilling Steinhagen's inequality with equality) as, e. g. evaluating (ub₃) at \mathbb{B} gives a value obviously bigger than 3.

It is also quite easy to see that for a pendant of our diagram for higher dimensional sets Steinhagen's inequality induces a facet.

Theorem 3.6. *Let $K \in \mathcal{K}^2$. Then*

$$(ub_3) \quad w(K) \leq 2r(K) \left(1 + \frac{2r(K)R(K)}{D(K)^2} \left(1 + \sqrt{1 - \left(\frac{D(K)}{2R(K)}\right)^2} \right) \right)$$

4. THE SKELETON OF THE 3-DIMENSIONAL DIAGRAM

This section is devoted to the description of the families of bodies filling the faces of $\text{bd}(f(\mathcal{K}^2))$. We start in Subsection 4.1 describing the sets fulfilling three or more inequalities with equality, the vertices of $\text{bd}(f(\mathcal{K}^2))$. In Subsection 4.2 we discuss the families of sets fulfilling two inequalities with equality, the edges of $\text{bd}(f(\mathcal{K}^2))$. Finally, in Subsection 4.3 the sets filling the different facets are explained. For the description of these sets we always assume that \mathbb{B} is the circumball, but for a better understanding of the geometric inequalities we will keep the value $R(K)$ in each description.

In case there does not exist a unique set, which is mapped to a boundary point of the diagram, we will usually describe in some way the range of sets mapped to that point, e. g. by giving maximal and minimal sets (with respect to set inclusion) if appropriate. However, as this is not our major topic, we neither claim completeness nor present proper proofs.

4.1. Vertices of the diagram. The vertices, including their radii, and for each the inequalities which are fulfilled with equality are listed in the following:

- \mathbb{B} Obviously, the *euclidean ball* \mathbb{B} is the unique set mapped to $f(\mathbb{B}) = (1, 1, 1)$ in the diagram. It is extreme for the inequalities (lb_1) , (ib_1) , (ub_1) , and (ib_2) .
- \mathbb{L} The radii of the *line segment* \mathbb{L} are easy to see, too: $f(\mathbb{L}) = (0, 0, 1)$ and also it is the only set mapped to this coordinates. The inequalities it fulfills with equality are (lb_1) , (lb_2) , (ib_1) , and (ub_3) . It also fulfills (ub_2) with equality, but this is an artefact which will be explained in Remark 4.1.
- $\mathbb{I}_{\pi/3}$ The radii of the *equilateral triangle* $\mathbb{I}_{\pi/3}$ are well known: $f(\mathbb{I}_{\pi/3}) = (1/2, 3/4, \sqrt{3}/2)$. It is the unique set with these coordinates and extreme for the inequalities (ub_1) , (ub_2) , (ub_3) , (lb_2) , and (ib_3) .
- \mathbb{RT} The *Reuleaux triangle* \mathbb{RT} is the intersection of three euclidean balls of radius $\sqrt{3}$ centered in the vertices of $\mathbb{I}_{\pi/3}$. On the one hand it has the same diameter and circumradius as $\mathbb{I}_{\pi/3}$. On the other hand it is of constant width, thus (lb_1) and (ib_2) imply $w(\mathbb{RT}) = r(\mathbb{RT}) + R(\mathbb{RT}) = D(\mathbb{RT})$. Hence $f(\mathbb{RT}) = (\sqrt{3} - 1, \sqrt{3}/2, \sqrt{3}/2)$ and \mathbb{RT} is the unique set mapped to this point of the diagram. It is extreme for the inequalities (ub_1) , (ib_2) and (ib_3) .
- $\mathbb{I}_{\pi/2}$ The *(isosceles) right-angled triangle* $\mathbb{I}_{\pi/2}$ (for short we will sometimes ommit the term “isosceles”) has diameter $D(\mathbb{I}_{\pi/2}) = 2R(\mathbb{I}_{\pi/2})$ and its width coincides with its height above the diameter edge, thus $w(\mathbb{I}_{\pi/2}) = R(\mathbb{I}_{\pi/2})$. Using the semiperimeter formula for triangles, we obtain that the inradius is

$$r(\mathbb{I}_{\pi/2}) = \frac{D(\mathbb{I}_{\pi/2})w(\mathbb{I}_{\pi/2})}{D(\mathbb{I}_{\pi/2}) + 2\sqrt{2}R(\mathbb{I}_{\pi/2})} = \frac{R(\mathbb{I}_{\pi/2})}{1 + \sqrt{2}} = (\sqrt{2} - 1)R(\mathbb{I}_{\pi/2}).$$

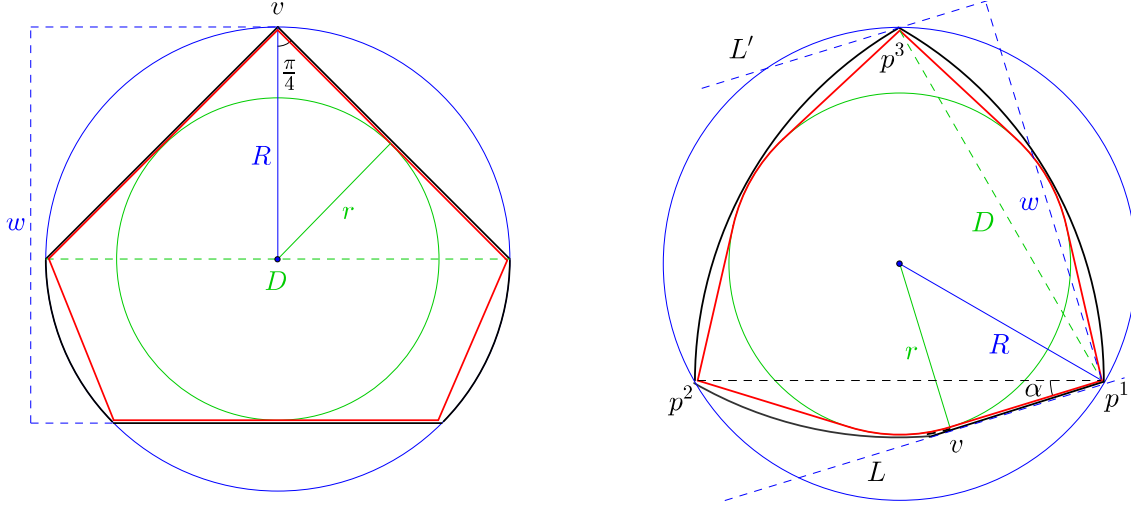
Thus $f(\mathbb{I}_{\pi/2}) = (\sqrt{2} - 1, 1/2, 1)$ and there is no different K mapped to this coordinates (as one may easily see in proceeding the construction of a set mapped to this coordinates). $\mathbb{I}_{\pi/2}$ is extreme for the inequalities (ub_2) , (ub_3) and (ib_1) .

- \mathbb{SB} The *(right-angled concentric) sailing boat* \mathbb{SB} is the intersection of \mathbb{B} and a homothetic of $\mathbb{I}_{\pi/2}$ with incenter at 0 and a vertex v located where the two edges of equal length intersect on \mathbb{S} (see Figure 3.1). Hence the in- and circumball of \mathbb{SB} are concentric and one can easily see from the construction, that $1/2 D(\mathbb{SB}) = \sqrt{2}r(\mathbb{SB}) = R(\mathbb{SB})$. Its width is attained in any of the orthogonal directions to any three of the edges of $\mathbb{I}_{\pi/2}$. Especially from measuring between v and its opposite edge, we obtain

$$w(\mathbb{SB}) = r(\mathbb{SB}) + R(\mathbb{SB}) = (1/\sqrt{2} + 1) R(\mathbb{SB}).$$

Thus $f(\mathbb{SB}) = (1/\sqrt{2}, 1/2(1/\sqrt{2} + 1), 1)$. The sailing boat fulfills inequalities (ub_1) , (ub_2) and (ib_1) with equality. Finally, denoting the (circumspherical) pentagon formed from the five vertices of \mathbb{SB} by \mathbb{CP} , we obtain $f(K) = f(\mathbb{SB})$ for any $K \in \mathcal{K}^2$, iff $\mathbb{CP} \subset K \subset \mathbb{SB}$.

- \mathbb{SR} The *sliced Reuleaux triangle* \mathbb{SR} is the intersection of a Reuleaux triangle \mathbb{RT} and a halfspace H which supports a vertex of \mathbb{RT} , say p^1 , and its inball in a point v (see Figure 3.2). By construction it keeps the same diameter, in- and circumradius as \mathbb{RT} . The width of \mathbb{SR} is attained between the parallel lines $L = \text{bd}(H)$, and L' supporting \mathbb{SR} in the vertex p^2 , which is furthest from v .



3.1: The sailing boat $\mathbb{S}\mathbb{B}$ in black and the pentagon $\mathbb{C}\mathbb{P}$ (sharing the vertices with $\mathbb{S}\mathbb{B}$) in red.

3.2: The sliced Reuleaux triangle $\mathbb{S}\mathbb{R}$ in black and $\mathbb{S}\mathbb{R}_{\min}$ (the minimal set sharing all radii with $\mathbb{S}\mathbb{R}$) in red.

FIGURE 3. Sailing boats and sliced Reuleaux triangles.

Defining α to be the angle between L and the line segment $[p^2, p^3]$, where p^3 is the remaining vertex of $\mathbb{I}_{\pi/3}$, one easily computes

$$r(\mathbb{S}\mathbb{R}) = R(\mathbb{S}\mathbb{R}) \sin(\pi/6 + \alpha) \quad \text{and} \quad w(\mathbb{S}\mathbb{R}) = D(\mathbb{S}\mathbb{R}) \cos(\pi/6 - \alpha).$$

Hence $\alpha = \arcsin(r(\mathbb{S}\mathbb{R})/R(\mathbb{S}\mathbb{R})) - \pi/6$ and thus

$$w(\mathbb{S}\mathbb{R}) = D(\mathbb{S}\mathbb{R}) \cos(\pi/3 - \arcsin(r(\mathbb{S}\mathbb{R})/R(\mathbb{S}\mathbb{R}))).$$

We obtain $f(\mathbb{S}\mathbb{R}) = (\sqrt{3} - 1, \sqrt{3}/2 \cos(\pi/3 - \arcsin(\sqrt{3} - 1)), \sqrt{3}/2)$ and extremality for the inequalities (lb_3) , (ib_2) and (ib_3) .

Denoting by $\mathbb{S}\mathbb{R}_{\min}$ the convex hull of the vertices and the inball of $\mathbb{R}\mathbb{T}$, one may easily verify that $f(K) = f(\mathbb{S}\mathbb{R})$ for any $K \in \mathcal{K}^2$, iff $\mathbb{S}\mathbb{R}_{\min} \subset K \subset \mathbb{S}\mathbb{R}$.

FR Let $\mathbb{F}\mathbb{R}$ be the *flattened Reuleaux triangle*, obtained by replacing two of the three edges of $\mathbb{I}_{\pi/3}$ by the according arcs of $\mathbb{R}\mathbb{T}$. It has the same circumradius, diameter and width than $\mathbb{I}_{\pi/3}$ and defining a to be the distance from the center of the inball to each vertex incident with the linear edge, it follows $a^2 = r(\mathbb{F}\mathbb{R})^2 + 1/4 D(\mathbb{F}\mathbb{R})^2$ and $D(\mathbb{F}\mathbb{R}) = a + r(\mathbb{F}\mathbb{R})$ (see Figure 4.1). Hence $4(D(\mathbb{F}\mathbb{R}) - r(\mathbb{F}\mathbb{R}))^2 = 4r(\mathbb{F}\mathbb{R})^2 + D(\mathbb{F}\mathbb{R})^2$ and, after dividing by $D(\mathbb{F}\mathbb{R})$, we obtain $3D(\mathbb{F}\mathbb{R}) = 8r(\mathbb{F}\mathbb{R})$. Thus $f(\mathbb{F}\mathbb{R}) = (\sqrt{27}/8, 3/4, \sqrt{3}/2)$ and equality holds in the inequalities (lb_2) , (lb_3) and (ib_3) .

Denoting the convex hull of $\mathbb{I}_{\pi/3}$ and the inball of $\mathbb{F}\mathbb{R}$ by $\mathbb{F}\mathbb{R}_{\min}$, it holds $f(K) = f(\mathbb{F}\mathbb{R})$, iff $\mathbb{F}\mathbb{R}_{\min} \subset K \subset \mathbb{F}\mathbb{R}$ (see Figure 4.1).

BT Let $p^1, p^2, p^3, p^4 \in \mathbb{S}$ be, s. t. $\text{conv}\{p^1, p^2, p^3, p^4\}$ is a trapezoid with $[p^1, p^2]$ the longer and $[p^3, p^4]$ the shorter parallel line, and s. t. $\text{conv}\{p^1, p^2, p^3\}$ as well as $\text{conv}\{p^1, p^2, p^4\}$ are isosceles triangles (the first with $[p^1, p^2]$, $[p^1, p^3]$ the edges of equal length, the second with $[p^1, p^2]$, $[p^2, p^4]$) and $\arcsin(3/4)$ in both cases the angle between the two equal edges (see Figure 4.2). We write $\mathbb{I}_{\arcsin(3/4)}$ for such an isosceles triangle (cf. Subsection 4.2). Substituting the edges $[p^1, p^4]$ and $[p^2, p^3]$ by two arcs of circumference of

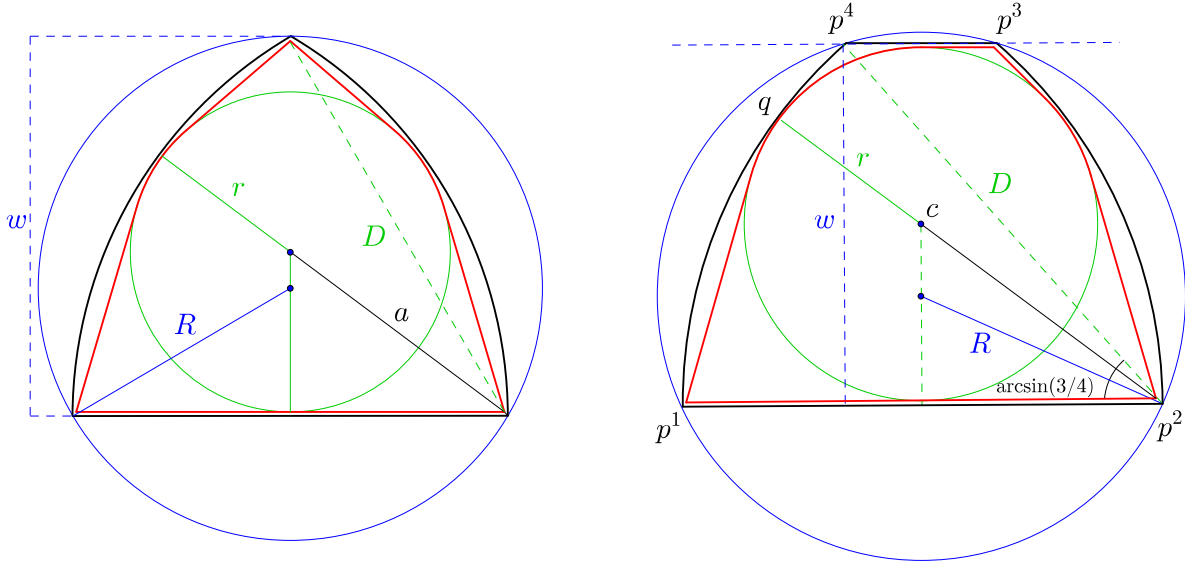
4.1: In black \mathbb{FR} , in red \mathbb{FR}_{\min} .4.2: In black \mathbb{BT} , in red \mathbb{BT}_{\min} .

FIGURE 4. The flattened Reuleaux triangle and the bent trapezoid.

radius $\|p^1 - p^2\| = D(I_{\arcsin(3/4)})$ and centers p^1 and p^2 , respectively, we obtain the *bent trapezoid* \mathbb{BT} .

By construction \mathbb{BT} and $I_{\arcsin(3/4)}$ have the same width w , diameter D , and circumradius $R = 1$. We prove that the inball of \mathbb{BT} is tangent to the two parallels and the two arcs: Let B be a ball of radius $r = 1/2 w$ and center $c = 1/4(p^1 + p^2 + p^3 + p^4)$, and denote the intersection point of the line through p^2 and c with the bow between p^1 and p^4 by q . We show that $\|c - q\| = r$ which then implies $r(\mathbb{BT}) = r$:

$$(i) \|c - q\| = D - \|c - p^2\|, \quad (ii) r^2 + 1/4 D^2 = \|c - p^2\|^2, \quad (iii) w = 3/4 D.$$

From (iii) we obtain $D = 8/3 r$, and using (i) combined with (ii) gives

$$\|c - q\| = D - \sqrt{r^2 + 1/4 D^2} = 8/3 r - \sqrt{r^2 + 16/9 r^2} = r,$$

as we wanted to show. Thus $r(\mathbb{BT}) = r = 1/2 w$.

For computing D , we use the fact that the line from p^2 through 0 is the bisecting line of the angle $\arcsin(3/4)$ between $[p^1, p^2]$ and $[p^2, p^4]$ at p^2 which means

$$\frac{D}{2R} = \frac{D(I_{\arcsin(3/4)})}{2R(I_{\arcsin(3/4)})} = \cos\left(\frac{1}{2} \arcsin\left(\frac{3}{4}\right)\right).$$

This implies

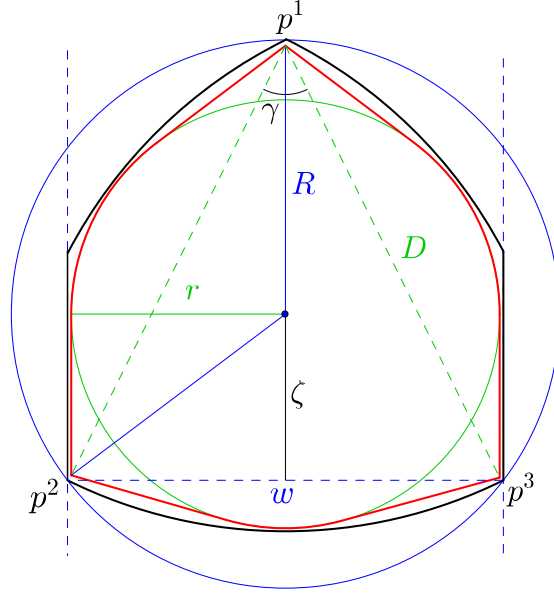
$$D = 2 \cos(1/2 \arcsin(3/4)) R = \sqrt{2 + \sqrt{7}/2} R,$$

and using the above properties on the radii of \mathbb{BT} we obtain that

$$2r = w = 3/4 D = 3/4 \sqrt{2 + \sqrt{7}/2} R.$$

Hence

$$f(\mathbb{BT}) = \left(3/8 \sqrt{2 + \sqrt{7}/2}, 3/8 \sqrt{2 + \sqrt{7}/2}, 1/2 \sqrt{2 + \sqrt{7}/2}\right),$$

FIGURE 5. The hood \mathbb{H} in black and \mathbb{H}_{\min} in red.

and one may easily check that it fulfills the inequalities (lb_1) , (lb_2) , and (lb_3) with equality.

Denoting the convex hull of p^1, p^2, p^3 and B by \mathbb{BT}_{\min} , it holds $f(K) = f(\mathbb{BT})$, iff $\mathbb{BT}_{\min} \subset K \subset \mathbb{BT}$ (cf. Figure 4.2).

\mathbb{H} The last vertex satisfies (lb_1) , (ib_2) and (lb_3) with equality, whereby its shape is determined as follows: from (lb_1) there must exist two parallel lines supporting the inball of the set and because of (ib_2) it must have concentric in- and circumball. The two parallels supporting the inball contain two separated arcs of the circumsphere between them. Let p^1, p^2, p^3 be points, s. t. p^2 and p^3 lie in one arc and each in one of the supporting lines, while p^1 lies in the other arc and at the same distance from p^2 and p^3 . Finally, we connect p^2 and p^3 by an arc centered in p^1 , its radius as well as the radius of the inball chosen, s. t. the arc is tangent to the inball (cf. Figure 5). The convex set bounded by the two supporting parallel lines and the three arcs with centers p^1, p^2, p^3 and radius $\|p^1 - p^2\|$ is called the **hood** and denoted by \mathbb{H} .

Remember that we always assume 0 to be the circumcenter and let γ be s. t. $I_\gamma = \text{conv}\{p^1, p^2, p^3\}$ is the isosceles triangle built by p^1, p^2, p^3 . Thus $R(\mathbb{H}) = R(I_\gamma)$, $D(\mathbb{H}) = D(I_\gamma) = r(\mathbb{H}) + R(\mathbb{H})$ and $2r(\mathbb{H}) = w(\mathbb{H})$.

For the computation of $r(\mathbb{H})$ let ζ denote the distance from 0 to $[p^2, p^3]$. Considering the two right-angled triangles $\text{conv}\{0, p^2, 1/2(p^2 + p^3)\}$ and $\text{conv}\{p^1, p^2, 1/2(p^2 + p^3)\}$ we obtain

$$(i) \quad r(\mathbb{H})^2 + \zeta^2 = R(\mathbb{H})^2 \quad \text{and} \quad (ii) \quad D(\mathbb{H})^2 = (\zeta + R(\mathbb{H}))^2 + r(\mathbb{H})^2$$

(cf. Figure 5). Solving (i) for ζ and inserting it into (ii), keeping into account that $D(\mathbb{H}) = r(\mathbb{H}) + R(\mathbb{H})$, we obtain

$$(r(\mathbb{H}) + R(\mathbb{H}))^2 = D(\mathbb{H})^2 = (\sqrt{R(\mathbb{H})^2 - r(\mathbb{H})^2} + R(\mathbb{H}))^2 + r(\mathbb{H})^2.$$

Solving for $r(\mathbb{H})$ gives the unique positive real solution

$$r(\mathbb{H}) = \left(\frac{1}{2} \sqrt{\varsigma + \xi} + \sqrt{-\varsigma - \xi + \frac{16}{\sqrt{\varsigma + \xi}} - 1} \right) R(\mathbb{H}),$$

where $\varsigma = 1/3(864 - 96\sqrt{69})^{1/3}$ and $\xi = 2(2/3)^{2/3}(9 + \sqrt{69})^{1/3}$. Thus

$$f(\mathbb{H}) = (r(\mathbb{H}), r(\mathbb{H}), 1/2(r(\mathbb{H}) + 1)) \approx (0.7935, 0.7935, 0.8967).$$

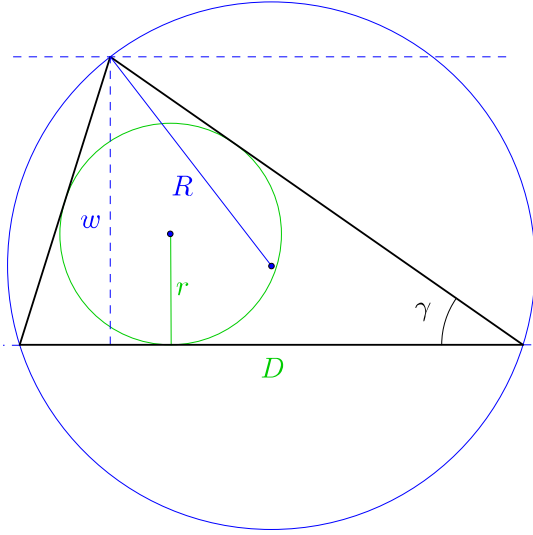
Denoting the convex hull of the inball of \mathbb{H} and p^1, p^2, p^3 , by \mathbb{H}_{\min} , it holds $f(K) = f(\mathbb{H})$, iff $\mathbb{H}_{\min} \subset K \subset \mathbb{H}$ (cf. Figure 5).

| Name | Symbol | Approximate Coordinates | $lb_{1,2,3}$ $ib_{1,2,3}$ $ub_{1,2,3}$ |
|-----------------------------|----------------------|--------------------------|--|
| Ball | \mathbb{B} | (1, 1, 1) | + - - + + - + - - |
| Equilateral triangle | $\mathbb{I}_{\pi/3}$ | (0.5, 0.75, 0.8660) | - + - - - + + + + |
| Line segment | \mathbb{L} | (0, 0, 1) | + + - + - - - \pm + |
| Reuleaux triangle | \mathbb{RT} | (0.7321, 0.8660, 0.8660) | - - - - + + + - - |
| Right-angled triangle | $\mathbb{I}_{\pi/2}$ | (0.4142, 0.5, 1) | - - - + - - - + + |
| Sailing boat | \mathbb{SB} | (0.7071, 0.8536, 1) | - - - + - - + + - |
| Sliced Reuleaux triangle | \mathbb{SR} | (0.7321, 0.8440, 0.8660) | - - + - + + - - - |
| Flattened Reuleaux triangle | \mathbb{FR} | (0.6495, 0.75, 0.8660) | - + + - - + - - - |
| Bent trapezoid | \mathbb{BT} | (0.6836, 0.6836, 0.9114) | + + + - - - - - - |
| Hood | \mathbb{H} | (0.7935, 0.7935, 0.8967) | + - + - + - - - - |

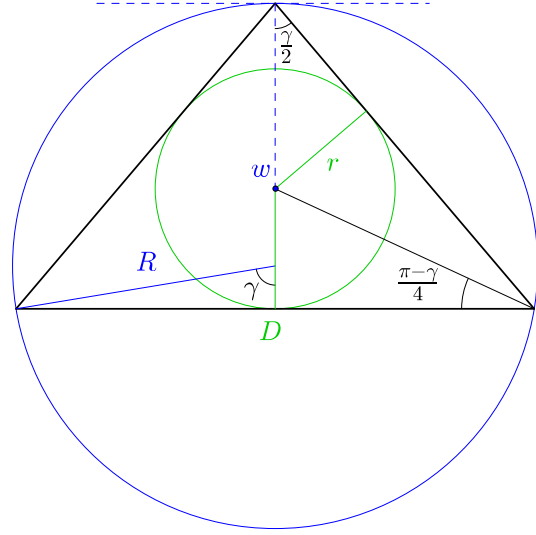
TABLE 1. The table lists the planar sets mapped to vertices of the 3-dimensional Blaschke-Santaló diagram, their (approximate) radii, and the inequalities they fulfill with equality (+) or not (-). The \pm for the line segment in the (ub_2) -column is explained in Remark 4.1

Remark 4.1. *Considering Table 1 we may observe the following: all inequalities besides (ub_3) are fulfilled with equality by exactly four vertices. Moreover, since all three vertices of (ub_3) also fulfill (ub_2) with equality (and since we will later prove these two inequalities more or less within one proof), we may understand them as one inequality in two parts. Doing so all inequalities are fulfilled by exactly four vertices, a fact which in a polytopal setting would be quite exceptional. (To be honest, accepting the two inequalities to be a joint one, the right-angled triangle would not be a vertex anymore due to our definition, but nevertheless we think the whole matter is remarkable.)*

4.2. Edges of the diagram. Next we give constructions of explicit families of convex sets mapped onto the intersection of two of the surfaces obtained from the equality cases of the inequalities collected in Section 3. In particular, every family of sets $\{K_t\}_{t \in [t_1, t_2]}$ described, induces a closed differentiable curve $f(\{K_t : t \in [t_1, t_2]\})$ in \mathbb{R}^3 . In our nomenclature they form the edges of the diagram. Each edge is named via its two endpoints, e. g. $(\mathbb{I}_{\pi/3}, \mathbb{B})$ denotes the edge between $\mathbb{I}_{\pi/3}$ and \mathbb{B} .



6.1: $I_\gamma, \gamma \in [0, \pi/3]$.



6.2: $I_\gamma, \gamma \in [\pi/3, \pi/2]$.

FIGURE 6. (Acute) isosceles triangles.

- (\mathbb{RT}, \mathbb{B}) It is a well known property that $w(K) = r(K) + R(K) = D(K)$, iff K is of constant width. Thus all *sets of constant width* fulfill (ub_1) and (ib_2) with equality. Essentially all edges with \mathbb{B} as an endpoint are real linear edges of the diagram: because of Lemma 2.1 we may pass the full edge from \mathbb{RT} to \mathbb{B} with *rounded Reuleaux triangles*, i. e. the outer parallel bodies $(1 - \lambda)\mathbb{RT} + \lambda\mathbb{B}$, $\lambda \in [0, 1]$ of the Reuleaux triangle.
- (\mathbb{L}, \mathbb{B}) Whenever K is *centrally symmetric* it satisfies the equations $D(K) = 2R(K)$ and $w(K) = 2r(K)$. Thus f maps K onto the linear edge formed from the equality cases of (lb_1) and (ib_1). Again, because of Lemma 2.1, the outer parallel bodies $(1 - \lambda)\mathbb{L} + \lambda\mathbb{B}$, $\lambda \in [0, 1]$, of \mathbb{L} (called *sausages*) already fill the whole edge.
- (\mathbb{SB}, \mathbb{B}) Lemma 2.1 implies that all *rounded sailing boats* $(1 - \lambda)\mathbb{SB} + \lambda\mathbb{B}$, $\lambda \in [0, 1]$ satisfy the inequalities (ub_1) and (ib_1) with equality and fill the corresponding edge of the diagram.
- (\mathbb{H}, \mathbb{B}) Because of Lemma 2.1 the *rounded hoods* $(1 - \lambda)\mathbb{H} + \lambda\mathbb{B}$, $\lambda \in [0, 1]$ satisfy the inequalities (lb_1) and (ib_2) with equality and their images through f fill the corresponding edge.
- ($\mathbb{L}, \mathbb{I}_{\pi/3}$) I_γ denotes an *isosceles triangle* with an angle γ between the two edges of equal length (see Figure 6.1). If $\gamma \in [0, \pi/3]$, the two edges of equal length attain its diameter $D = D(I_\gamma) = 2R \cos(\gamma/2)$, where $R = R(I_\gamma) = 1$. Abbreviating also $r = r(I_\gamma)$ and $w = w(I_\gamma)$, it was shown in [13] and [17] that

$$\left(2 + \sqrt{4 - (D/R)^2}\right) r = w \quad \text{and} \quad 2wR = D^2 \sqrt{4 - (D/R)^2}.$$

- Thus one may check that I_γ fulfills (ub_3) and (lb_2) with equality for any $\gamma \in [0, \pi/3]$.
- ($\mathbb{I}_{\pi/2}, \mathbb{I}_{\pi/3}$) Consider the family of *isosceles triangles* I_γ as described above, but now with $\gamma \in [\pi/3, \pi/2]$. Obviously their diameter $D(I_\gamma)$ is attained by the edge opposite to γ . Using Lemma 1.3 we obtain that the angle at the circumcenter between the height onto the diametral edge and the radiusline from the center to one of the diametral vertices is

again γ (cf. Figure 6.2). The width is obviously attained orthogonal to the diametral edge and thus it is the sum of the inradius and the distance from the incenter to the opposing vertex. Considering the right angled triangle with the incenter, the midpoint of the diametral edge, and one of its endpoints as vertices, it is easy to check that the interior angle in that endpoint is $(\pi-\gamma)/4$. Hence $2r(I_\gamma) = D(I_\gamma) \tan((\pi-\gamma)/4)$ and using trigonometric identities it follows

$$\tan\left(\frac{\pi-\gamma}{4}\right) = \frac{1-\cos((\pi-\gamma)/2)}{\sin((\pi-\gamma)/2)} = \frac{1-\sin(\gamma/2)}{\cos(\gamma/2)}.$$

Altogether, omitting arguments we have

$$D = 2R \sin(\gamma), \quad w = r \left(1 + \frac{1}{\sin(\gamma/2)}\right), \quad \text{and}$$

$$r = \frac{D}{2} \left(\frac{1}{\cos(\gamma/2)} - \tan\left(\frac{\gamma}{2}\right)\right).$$

Finally, again using trigonometric identities, we may remove γ from the width formula in two ways

$$\begin{aligned} w &= r \left(1 + \frac{1}{\sin(\gamma/2)}\right) = r \left(1 + \sqrt{\frac{2}{1-\cos(\gamma)}}\right) \\ &= r \left(1 + \frac{\sqrt{2}}{\sin(\gamma)} \sqrt{1+\cos(\gamma)}\right) = r \left(1 + \frac{2\sqrt{2}R}{D} \sqrt{1 + \sqrt{1 - \left(\frac{D}{2R}\right)^2}}\right) \end{aligned}$$

or

$$\begin{aligned} &= r \left(1 + \frac{1}{\sin(\gamma/2)}\right) = 2r \left(1 + \frac{1}{2} \left(\frac{1}{\sin(\gamma/2)} - 1\right)\right) = 2r \left(1 + \frac{1/\cos(\gamma/2) - \tan(\gamma/2)}{2 \tan(\gamma/2)}\right) \\ &= 2r \left(1 + \frac{r}{D \tan(\gamma/2)}\right) = 2r \left(1 + \frac{r(1+\cos(\gamma))}{D \sin(\gamma)}\right) \\ &= 2r \left(1 + \frac{2rR}{D^2} \left(1 + \sqrt{1 - \left(\frac{D}{2R}\right)^2}\right)\right). \end{aligned}$$

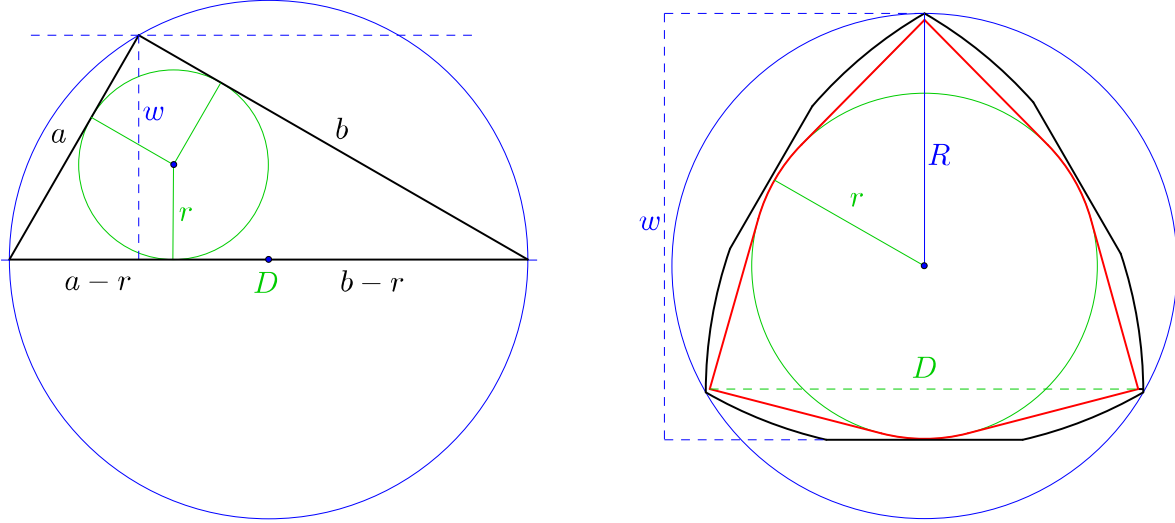
proving that I_γ , $\gamma \in [\pi/3, \pi/2]$ is extreme for (ub_2) and (ub_3) .

$(\mathbb{L}, \mathbb{I}_{\pi/2})$ The next family we consider are the *right-angled triangles* $\mathbb{T}_r^{\pi/2}$, where $r \in [0, r(\mathbb{I}_{\pi/2})]$ denotes their inradius. Naming the edges as their lengths a, b and $D = D(\mathbb{T}_r^{\pi/2}) = 2R(\mathbb{T}_r^{\pi/2})$, abbreviating $w = w(\mathbb{T}_r^{\pi/2})$ and recognizing that the inball touches D , s. t. it is split into two segments of lengths $a-r$ and $b-r$ (see Figure 7.1), we easily see that the perimeter p of $\mathbb{T}_r^{\pi/2}$ is $2r + 2D$ (or $2r + 4R$). Thus using the semiperimeter formular for the width, we obtain

$$wD = 2A = rp = 2r(r + D).$$

One may easily calculate that the right-angled triangles are extreme for the inequalities (ub_3) and (ib_1) .

$(\mathbb{I}_{\pi/3}, \mathbb{RT})$ For any $r \in [r(\mathbb{I}_{\pi/3}), r(\mathbb{RT})]$ we call $\mathbb{RB}_r = (r/r(\mathbb{I}_{\pi/3}) \mathbb{I}_{\pi/3}) \cap \mathbb{RT}$ a *Reuleaux blossom*, s. t. $\mathbb{RB}_{r(\mathbb{I}_{\pi/3})} = \mathbb{RB}_{1/2} = \mathbb{I}_{\pi/3}$ and $\mathbb{RB}_{r(\mathbb{RT})} = \mathbb{RB}_{\sqrt{3}-1} = \mathbb{RT}$ (see Figure 7.2). Obviously $r(\mathbb{RB}_r) = r$, $D(\mathbb{RB}_r) = \sqrt{3}R(\mathbb{RB}_r)$, and $w(\mathbb{RB}_r) = r + R(\mathbb{RB}_r)$. Hence they are extreme for the inequalities (ub_1) and (ib_3) .



7.1: $\mathbb{T}_r^{\pi/2}$.

7.2: In black RB_r , and in red a Yamanouti set with the same radii.

FIGURE 7. A right-angled triangle and a Reuleaux blossom.

A *Yamanouti set* of inradius r is mapped onto the same coordinates in the 3-dimensional Blaschke-Santaló diagram as the Reuleaux blossom RB_r . They are the convex hull of $\mathbb{I}_{\pi/3}$ and the intersection of three balls with centers in the vertices of $\mathbb{I}_{\pi/3}$ and radius taken in $[w(\mathbb{I}_{\pi/3}), w(\mathbb{RT})]$ (see [17] and cf. Figure 7.2). While the Yamanouti set is a unique minimal set (with respect to set inclusion) mapped to these coordinates, the corresponding Reuleaux Blossom is maximal but not unique (as one may support the inball in different points than the chosen ones). However, the Reuleaux blossoms are the only maximizers which possess the same symmetry group as $\mathbb{I}_{\pi/3}$.

($\mathbb{I}_{\pi/3}, \mathbb{SB}$) Let $\gamma \in [\pi/3, \pi/2]$ and c the incenter of \mathbb{I}_γ . Now rescale $\mathbb{I}_\gamma - c$ by a factor ρ , s. t. the vertex p of $\rho(\mathbb{I}_\gamma - c)$ between the two edges of equal length touches the boundary of \mathbb{B} . Then the *concentric sailing boat* is defined as $\text{SB}_\gamma^\circ = \rho(\mathbb{I}_\gamma - c) \cap \mathbb{B}$ (see Figure 8.1). Obviously, $R = R(\text{SB}_\gamma^\circ) = 1$ and $D = D(\text{SB}_\gamma^\circ) = D(\mathbb{I}_\gamma) = R \sin(\gamma)$. Moreover, since SB_γ° is concentric and the distance of the center from p is R we obtain

$$r = r(\text{SB}_\gamma^\circ) = R \sin\left(\frac{\gamma}{2}\right) \quad \text{and} \quad w = r + R = r \left(1 + \frac{1}{\sin(\gamma/2)}\right)$$

However, since $D = R \sin(\gamma)$ it follows exactly in the same ways as shown for $w(\mathbb{I}_\gamma)$ in the $(\mathbb{I}_{\pi/3}, \mathbb{I}_{\pi/2})$ -edge that

$$w = r \left(1 + \frac{1}{\sin(\gamma/2)}\right) = 2r \left(1 + \frac{2rR}{D^2} \left(1 + \sqrt{1 - \left(\frac{D}{2R}\right)^2}\right)\right).$$

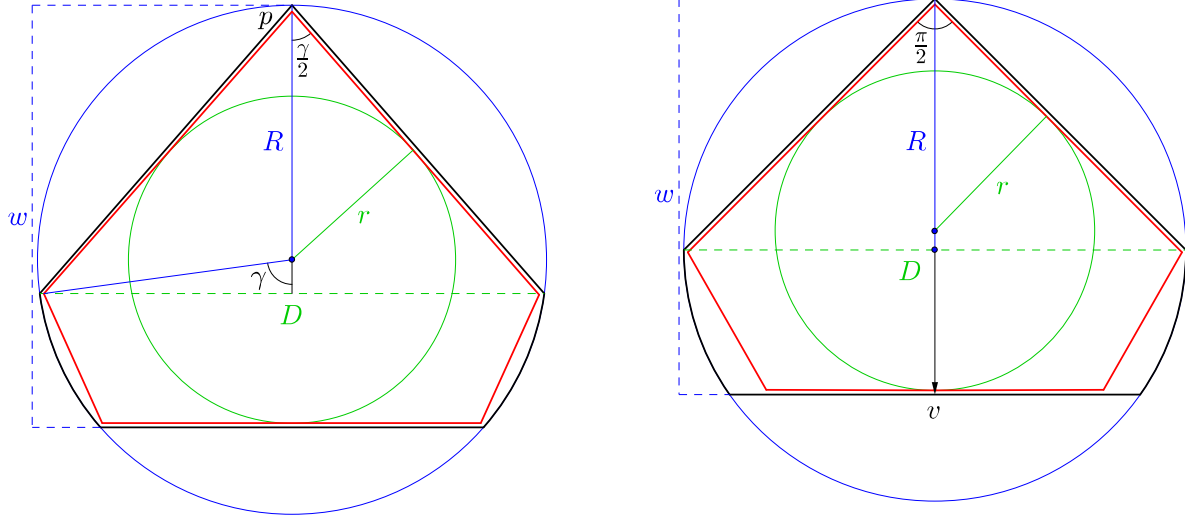
8.1: In black SB_γ° , in red the pentagon CP_γ° .8.2: In black $\text{SB}_{r, \pi/2}$, in red the pentagon $\text{SB}_{r, \pi/2}^{\min}$ in case that $w(\text{SB}_{r, \pi/2}) > \sqrt{2}R(\text{SB}_{r, \pi/2})$.

FIGURE 8. A concentric and a right-angled sailing boat.

Hence the concentric sailing boats are extreme for the inequalities (ub_1) and (ub_2) . Denoting the concentric pentagon built from the vertices of SB_γ° by CP_γ° , it holds $f(K) = f(\text{SB}_\gamma^\circ)$, iff $\text{CP}_\gamma^\circ \subset K \subset \text{SB}_\gamma^\circ$ (cf. Figure 8.1).

$(\mathbb{I}_{\pi/2}, \mathbb{SB})$ Let $r \in [r(\mathbb{I}_{\pi/2}), r(\mathbb{SB})]$ and $v \in \mathbb{R}^2$, s. t. the vertex of $v + (r/r(\mathbb{I}_{\pi/2}))\mathbb{I}_{\pi/2}$ between the two edges of equal length belongs to \mathbb{S} and the edges of equal length induce equal caps in \mathbb{B} (cf. Figure 8.2). Then $\text{SB}_{r, \pi/2} = (v + (r/r(\mathbb{I}_{\pi/2}))\mathbb{I}_{\pi/2}) \cap \mathbb{B}$ is a *right-angled sailing boat*. Hence $D(\text{SB}_{r, \pi/2}) = 2R(\text{SB}_{r, \pi/2})$, $r(\text{SB}_{r, \pi/2}) = r(v + (r/r(\mathbb{I}_{\pi/2}))\mathbb{I}_{\pi/2}) = r$, and $w(\text{SB}_{r, \pi/2}) = r/r(\mathbb{I}_{\pi/2})w(\mathbb{I}_{\pi/2}) = (\sqrt{2} + 1)r$. Thus they are extreme for the inequalities (ub_2) and (ib_1) and it holds $K \subset \text{SB}_{r, \pi/2}$ for any set K with $f(K) = f(\text{SB}_{r, \pi/2})$. Concerning possible minimal sets mapped to the same coordinates in the diagram, let $p^1, p^2, p^3 \in \mathbb{S}$, s. t. $\text{conv}\{p^1, p^2, p^3\} = \mathbb{I}_{\pi/2}$, with the right-angle at p^3 . Now, if $w(\text{SB}_{r, \pi/2}) \leq \sqrt{2}R(\text{SB}_{r, \pi/2})$, the set $\text{SB}_{r, \pi/2}^{\min} := \text{conv}(\mathbb{I}_{\pi/2}, (p^3 + w(\text{SB}_{r, \pi/2})\mathbb{B}) \cap \text{SB}_{r, \pi/2})$ fulfills $\text{SB}_{r, \pi/2}^{\min} \subset K$, for all K with $f(K) = f(\text{SB}_{r, \pi/2})$. In case of $w(\text{SB}_{r, \pi/2}) > \sqrt{2}R(\text{SB}_{r, \pi/2})$ (i. e. $r > (2 - \sqrt{2})R(\text{SB}_{r, \pi/2})$), call L the supporting line to the inball in v , and let $p^4, p^5 \in L$ at distance $w(\text{SB}_{r, \pi/2})$ from the segments $[p^1, p^3]$, $[p^2, p^3]$, respectively. Then the pentagon $\text{SB}_{r, \pi/2}^{\min} := \text{conv}\{p^i, i \in [5]\}$ is a minimal set mapped to the same coordinates as $\text{SB}_{r, \pi/2}$. However, one should recognize that $\text{SB}_{r, \pi/2}^{\min}$ is only one (maybe the “nicest”) possible choice for such a set (cf. Figure 8.2).

$(\mathbb{I}_{\pi/3}, \mathbb{FR})$ For any $r \in [r(\mathbb{I}_{\pi/3}), r(\mathbb{FR})]$ there exists $c \in \mathbb{R}^2$, s. t. $c + r\mathbb{B}$ is contained in \mathbb{FR} (by definition of inradius) and tangent to the linear edge of \mathbb{FR} (cf. Figure 9). Assuming c to be equidistant from the endpoints of that linear edge the sets $\text{BI}_{r, \pi/3} = \text{conv}(\mathbb{I}_{\pi/3}, v + r\mathbb{B})$, $r \in [r(\mathbb{I}_{\pi/3}), r(\mathbb{FR})]$ are called *bent equilaterals* and they satisfy $r(\text{BI}_{r, \pi/3}) = r$,

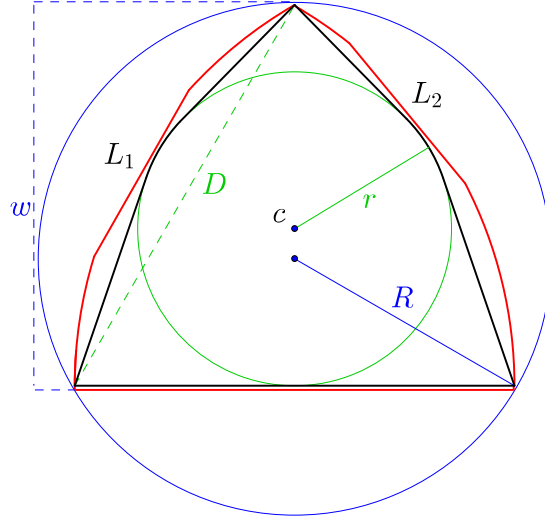


FIGURE 9. In black a bent equilateral $\text{BI}_{r, \pi/3}$, $r \in [r(\mathbb{I}_{\pi/3}), r(\mathbb{FR})]$ (for which all radii keep constant moving the inball horizontally), in red one possible maximal set containing $\text{BI}_{r, \pi/3}$.

$D(\text{BI}_{r, \pi/3}) = \sqrt{3}R(\text{BI}_{r, \pi/3})$ and $w(\text{BI}_{r, \pi/3}) = w(\mathbb{I}_{\pi/3})$. Thus the bent equilaterals with $r \in [r(\mathbb{I}_{\pi/3}), r(\mathbb{FR})]$ are extreme for the inequalities (lb_2) and (ib_3) .

With respect to set inclusion $\text{BI}_{r, \pi/3}$ is a minimal set mapped onto these coordinates. However, since there is some freedom in placing c , it is not a unique minimal set.

Choosing two common supporting half-spaces H_i , $i = 1, 2$ of $\text{BI}_{r, \pi/3}$ and its inball, s. t. $c + r\mathbb{B}$ is the inball of $\mathbb{FR} \cap H_1 \cap H_2$, one gets a maximal set containing $\text{BI}_{r, \pi/3}$ (but neither the choice of the half-spaces H_i , $i = 1, 2$ is unique nor is the choice of c , cf. Figure 9).

(\mathbb{FR}, SR) On the contrary, for any $r \in [r(\mathbb{FR}), r(\mathbb{SR})]$, let $c \in \mathbb{R}^2$, s. t. $c + r\mathbb{B}$ is tangent to the two (non-linear) arcs of \mathbb{FR} (see Figure 10.2). Then we define the *maximally-sliced Reuleaux triangle* SR_{r, w_r} to be the intersection of \mathbb{RT} with a halfspace supporting $c + r\mathbb{B}$ and containing a vertex of \mathbb{FR} , which is adjacent to its linear edge, on the boundary line of the halfspace. Abbreviating $D = D(\text{SR}_{r, w_r})$ and $R = R(\text{SR}_{r, w_r}) = 1$ again, it holds $r(\text{SR}_{r, w_r}) = r$ and $D = \sqrt{3}R$. Considering the angles α, β, γ inside SR_{r, w_r} (as given in Figure 10.2), we have

$$(i) \cos(\alpha) = D/2(D-r), \quad (ii) \sin(\alpha + \beta) = r/(D-r), \quad (iii) \cos(\gamma) = w/D.$$

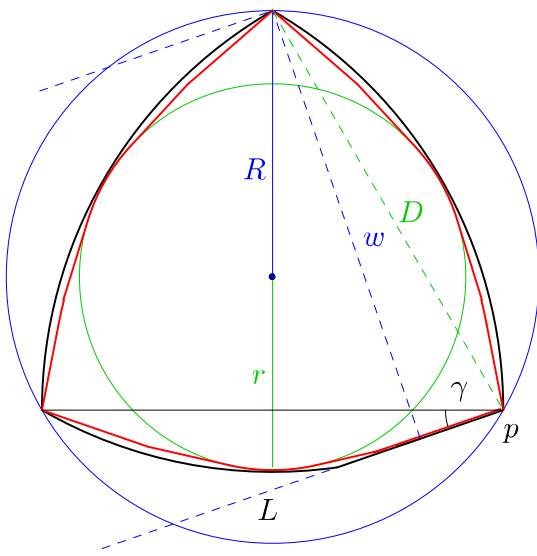
Passing (i) into (ii) one obtains

$$\beta = \arcsin\left(\frac{r}{D-r}\right) - \arccos\left(\frac{D}{2(D-r)}\right)$$

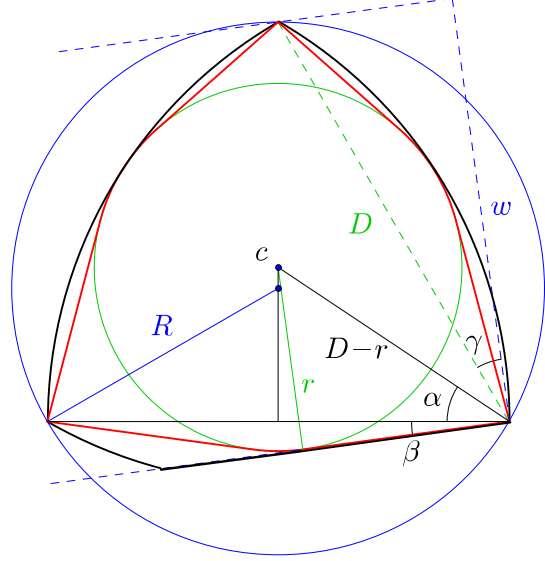
and since $\gamma = \pi/6 - \beta$ it follows from (iii) for the width $w = w(\text{SR}_{r, w_r})$ that

$$w = D \cos\left(\frac{\pi}{6} - \arcsin\left(\frac{r}{D-r}\right) + \arccos\left(\frac{D}{2(D-r)}\right)\right)$$

The sliced Reuleaux triangles fulfill inequalities (lb_3) and (ib_3) with equality. Moreover, denoting $\text{BI}_{r, \pi/3} := \text{conv}(\mathbb{I}_{\pi/3}, c + r\mathbb{B})$, with $r \in [r(\mathbb{FR}), r(\mathbb{SR})]$ again a *bent equilateral* it holds $f(K) = f(\text{SR}_{r, w_r})$, iff $\text{BI}_{r, \pi/3} \subset K \subset \text{SR}_{r, w_r}$ (cf. Figure 10.2).



10.1: In black a concentric sliced Reuleaux triangle SR_γ° and in red BY_γ .



10.2: In black a maximally-sliced Reuleaux triangle $\text{SR}_{r,w,r}$, in red a bent equilateral $\text{BI}_{r,\pi/3}$, $r \in [r(\mathbb{FR}), r(\mathbb{SR})]$.

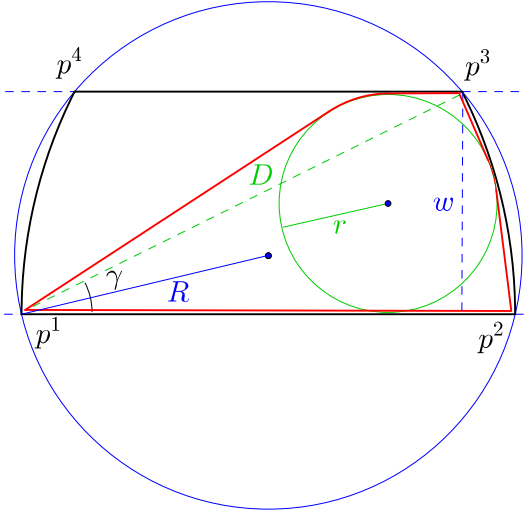
FIGURE 10. Sliced Reuleaux triangles

(SR, RT) Let L be a line containing a vertex of RT , say p , not cutting the interior of the inball of RT , and $\gamma \in [\arcsin(\sqrt{3}-1) - \pi/6, \pi/6]$ the angle between L and one of the segments joining p with one of the other two vertices (see Figure 10.1). The family of *concentric sliced Reuleaux triangles* SR_γ° are obtained from intersecting RT with the halfspace induced by L . The concentric sliced Reuleaux triangles have the same diameter, in-, and circumradius as RT , while the width is attained in the orthogonal direction to the line L . Hence $w(\text{SR}_\gamma^\circ) = D(\text{RT}) \sin(\pi/3 + \gamma)$. Concentric sliced Reuleaux triangles are extreme for the inequalities (ib_2) and (ib_3) .

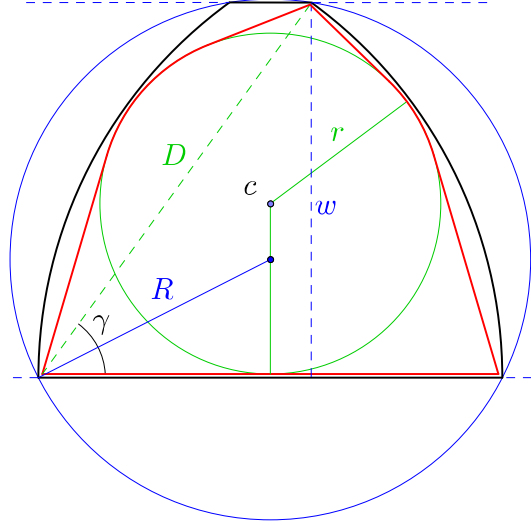
Denoting the convex hull of $r(\text{SR}_\gamma^\circ)\mathbb{B}$ and the Yamanouti set sharing width, diameter and circumradius with SR_γ° by BY_γ , then we have $f(K) = f(\text{SR}_\gamma^\circ)$, iff $\text{BY}_\gamma \subset K \subset \text{SR}_\gamma^\circ$ (see Figure 10.1).

(\mathbb{L}, BT) The construction of the sets in this edge is a generalization of that of the bent trapezoid BT in Subsection 4.1. Let $\text{I}_\gamma = \text{conv}\{p^1, p^2, p^3\}$ with $\gamma \in [0, \arcsin(3/4)]$, s. t. γ is the angle at p^1 . Moreover let $p^4 \neq p^3$ in the circumsphere of I_γ , s. t. $\text{conv}\{p^1, p^2, p^4\}$ is congruent with $\text{conv}\{p^1, p^2, p^3\}$ and possesses its angle γ at p^2 . Substituting the two edges $[p^1, p^4]$ and $[p^2, p^3]$ by two arcs of radius $D(\text{I}_\gamma)$ whose centers are p^1 and p^2 , respectively, the resulting set is a (*general*) *bent trapezoid* BT_γ , $\gamma \in [0, \arcsin(3/4)]$ (see Figure 11.1). It holds $D(\text{BT}_\gamma) = D(\text{I}_\gamma) = 2R(\text{I}_\gamma) \cos(\gamma/2)$ and $w(\text{BT}_\gamma) = w(\text{I}_\gamma) = D(\text{I}_\gamma) \sin(\gamma)$ and since they possess two parallel edges touching the inball in antipodal points $w(\text{BT}_\gamma) = 2r(\text{BT}_\gamma)$.

The bent trapezoids are extreme for the inequalities (lb_1) and (lb_2) . While BT_γ is the unique maximal set with respect to set inclusion, which is mapped onto these coordinates in the diagram, there does not exist a unique minimal set. Essentially, the convex hull of I_γ and any of the possible inballs of BT_γ shares all four radii with BT_γ and is minimal in that sense.



11.1: In black BT_γ with $\gamma < \arcsin(3/4)$, in red a minimal set whose inball is tangent to one of the curved edges of BT_γ .



11.2: In black BT_γ with $\gamma > \arcsin(3/4)$, in red an according bent isosceles.

FIGURE 11. Bent trapezoids.

(BT, FR) Adopting the construction of the bent trapezoids with $\gamma \in [0, \arcsin(3/4)]$ above, we define the *(general) bent trapezoid* BT_γ with $\gamma \in [\arcsin(3/4), \pi/3]$ (see Figure 11.1). They keep $D(\text{BT}_\gamma) = D(\text{I}_\gamma) = 2R(\text{I}_\gamma) \cos(\gamma/2)$, and $w(\text{BT}_\gamma) = w(\text{I}_\gamma) = D(\text{I}_\gamma) \sin(\gamma)$, but in difference to the bent trapezoids before, those with $\gamma > \arcsin(3/4)$ have an inball touching the two arcs of circumference and only the longer of the parallels. Thus it holds $1/4 D(\text{BT}_\gamma)^2 + r(\text{BT}_\gamma)^2 = (D(\text{BT}_\gamma) - r(\text{BT}_\gamma))^2$ from which we obtain $3/4 D(\text{BT}_\gamma)^2 - 2D(\text{BT}_\gamma)r(\text{BT}_\gamma) = 0$ or $8r(\text{BT}_\gamma) = 3D(\text{BT}_\gamma)$. Hence, the sets BT_γ , $\gamma \in [\arcsin(3/4), \pi/3]$, fulfill inequalities (lb_2) and (lb_3) with equality.

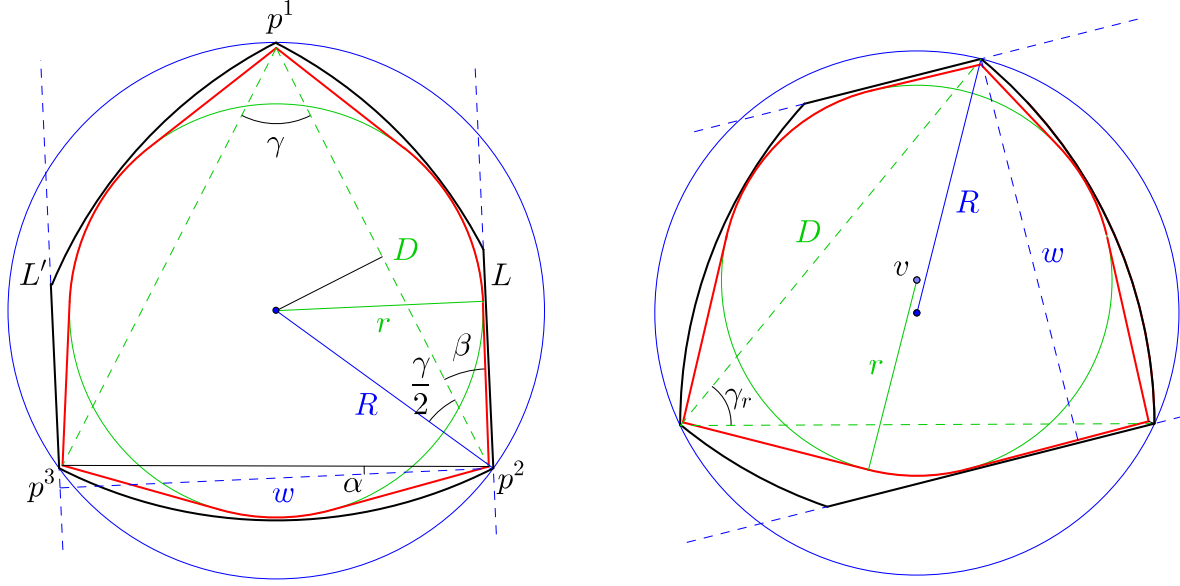
While BT_γ is the unique maximal set with respect to set inclusion, the bent isosceles given by the convex hull of one of the two possible copies of I_γ inside BT_γ and the inball of BT_γ is a minimal set with respect to set inclusion mapped to the same coordinates, which is unique (up to mirroring along the symmetry axis of BT_γ , cf. Figure 11.2).

(SR, H) Now, we generalize the hood \mathbb{H} as constructed in Subsection 4.1: For any $\gamma \in [2 \arcsin(r(\mathbb{H})/D(\mathbb{H})), \pi/3]$ let $\text{I}_\gamma = \text{conv}\{p^1, p^2, p^3\}$ with $D(\text{I}_\gamma) = \|p^1 - p^2\| = \|p^1 - p^3\|$ and define the space contained between

- the arcs with centers in the vertices of I_γ and radius $D(\text{I}_\gamma)$,
 - a line L through p^2 supporting the ball $(D(\text{I}_\gamma) - R(\text{I}_\gamma))\mathbb{B}$ and the smaller angle β between it and $[p^1, p^2]$, as well as
 - the parallel line L' to L supporting I_γ in p^3 ,
- as the *(general) hood* H_γ (see Figure 12.1).

One can easily see that $D(\text{H}_\gamma) = D(\text{I}_\gamma) = 2R(\text{I}_\gamma) \cos(\gamma/2)$ and $r(\text{H}_\gamma) = D(\text{H}_\gamma) - R(\text{H}_\gamma)$.

Observing that the angle between $[p^1, p^2]$ and $[0, p^2]$ in p^2 is $\gamma/2$ let α be the angle between $[p^2, p^3]$ and the perpendicular of L and $\beta = \gamma/2 - \alpha$ the angle between $[p^1, p^2]$



12.1: In black a general hood H_γ , in red a bent isosceles.

12.2: In black a bent pentagon BP_{r, γ_r} and in red a bent isosceles BI_{r, γ_r} , $r \in [r(\mathbb{BT}), r(\mathbb{H})]$.

FIGURE 12. Sets from the two edges meeting in \mathbb{H} and bounding (lb_3) .

and L , both in p^2 . Then, omitting the argument H_γ , we get

$$\begin{aligned} \text{(i)} \quad D &= 2R \cos(\gamma/2), & \text{(ii)} \quad r &= R \sin(\gamma/2 + \beta) = R \sin(\gamma - \alpha) \\ \text{(iii)} \quad w &= \|p^2 - p^3\| \cos(\alpha) = 2D \sin(\gamma/2) \cos(\alpha). \end{aligned}$$

From (i) and (ii) one immediately obtains $\gamma/2 = \arccos(D/2R)$ and $\alpha = \gamma - \arcsin(r/R)$. Thus (iii) can be rewritten as

$$\begin{aligned} w &= 2D \sin(\arccos(D/2R)) \cos(\gamma - \arcsin(r/R)) \\ &= 2D \sqrt{1 - \left(\frac{D}{2R}\right)^2} \cos\left(2 \arccos\left(\frac{D}{2(D-r)}\right) - \arcsin\left(\frac{r}{D-r}\right)\right). \end{aligned}$$

The hoods H_γ with $\gamma \in [2 \arcsin(r(\mathbb{H})/D(\mathbb{H})), \pi/3]$, are extreme for the inequalities (lb_3) and (ib_2) . While H_γ is maximal with respect to set inclusion, the bent isosceles $\text{conv}(I_\gamma, (D(H_\gamma) - R(H_\gamma))\mathbb{B})$ is minimal sharing all radii with H_γ (see Figure 12.1).

(\mathbb{BT}, \mathbb{H}) Let $r \in [r(\mathbb{BT}), r(\mathbb{H})]$ and γ_r the maximal $\gamma \in [0, \pi/3]$, s. t. we can find $c \in \mathbb{R}^2$ for which

- (i) $c + r\mathbb{B}$ is tangent to the two arcs of circumference with centers p^1 and p^2 and radius $D(I_{\gamma_r})$ above the segments $[p^2, p^3]$ and $[p^1, p^3]$, respectively, as well as
- (ii) two parallel lines L and L' both supporting $c + r\mathbb{B}$, support I_{γ_r} in, respectively, p^2 and p^3 (cf. Figure 12.2).

The *bent pentagon* BP_{r, γ_r} is defined as the space contained between the lines L, L' and the three arcs with radius $D(I_{\gamma_r})$ around the vertices of I_{γ_r} . They satisfy $D(BP_{r, \gamma_r}) = D(I_{\gamma_r}) = 2R(I_{\gamma_r}) \cos(\gamma_r/2)$, $r(BP_{r, \gamma_r}) = r$, and $w(BP_{r, \gamma_r}) = 2r(BP_{r, \gamma_r})$ and are extreme for the inequalities (lb_1) and (lb_3) .

Defining the bent isosceles $BI_{r, \gamma_r} := \text{conv}(I_{\gamma_r}, c + r\mathbb{B})$ (as we will do for (lb_2)), we obtain $f(K) = f(BP_{r, \gamma_r})$, iff $BI_{r, \gamma_r} \subset K \subset BP_{r, \gamma_r}$.

4.3. Facets of the diagram. In this section families of sets \mathcal{K}^2 are described for each of the inequalities stated in Section 3, s. t. for every point $x \in [0, 1]^3$ in the induced facet, there exists a set K_x within the family with $f(K_x) = x$.

(*lb*₁) Due to Lemma 2.1, all outer parallel bodies K of the bent trapezoids BT_γ of the $(\mathbb{L}, \mathbb{BT})$ -edge and the bent pentagons $\text{BP}_{r,\gamma}$ of the $(\mathbb{BT}, \mathbb{H})$ -edge fulfill the equation

$$2r(K) = w(K).$$

This means (*lb*₁) induces a linear facet of the diagram, which is bounded by the edges $(\mathbb{L}, \mathbb{BT})$ (bent trapezoids with $\gamma \leq 3/4$), $(\mathbb{BT}, \mathbb{H})$ (bent pentagons), (\mathbb{L}, \mathbb{B}) (sausages) and (\mathbb{H}, \mathbb{B}) (rounded hoods).

(*ib*₁) If K is an outer parallel body of a right-angled triangle $\text{T}_r^{\pi/2}$ or a right-angled sailing-boat $\text{SB}_{r,\pi/2}$ as described in Section 4.2, then Lemma 2.1 ensures

$$D(K) = 2R(K),$$

which means equality in (*ib*₁). Hence it is a linear facet of the diagram bounded by the edges (\mathbb{L}, \mathbb{B}) (sausages), $(\mathbb{L}, \mathbb{I}_{\pi/2})$ (right-angled triangles), $(\mathbb{I}_{\pi/2}, \mathbb{SB})$ (right-angled sailing-boats), and $(\mathbb{SB}, \mathbb{B})$ (rounded sailing boats).

To both facets, (*lb*₁) and (*ib*₁), much more sets are mapped. Remember that, e. g., all symmetric sets are mapped to the edge obtained from the intersection of the two facets.

(*ub*₁) Because of Lemma 2.1 and Lemma 2.3 any outer parallel body K of a Reuleaux blossom RB_r or a concentric sailing boat SB_γ^\odot , as well as any of the sets $K_\lambda := \lambda K + (1-\lambda)C_K$, $\lambda \in [0, 1]$, where C_K is a Scott-completion of a concentric sailing boat SB_γ^\odot fulfills $w(K) = r(K) + R(K)$. Thus (*ub*₁) defines a linear facet of the diagram, bounded by the edges $(\mathbb{I}_{\pi/3}, \mathbb{RT})$ (Reuleaux blossoms) and $(\mathbb{RT}, \mathbb{B})$ (rounded Reuleaux triangles), as well as $(\mathbb{I}_{\pi/3}, \mathbb{SB})$ (concentric sailing boats) and $(\mathbb{SB}, \mathbb{B})$ (rounded sailing boats).

(*ib*₂) Lemma 2.1 ensures that any outer parallel body K of a general hood H_γ or a concentric sliced Reuleaux triangle SR_γ^\odot fulfills

$$D(K) = r(K) + R(K),$$

filling the linear facet from the star-shapedness with respect to \mathbb{B} . Moreover, the sets $K_\lambda := \lambda K + (1-\lambda)C_K$, $\lambda \in [0, 1]$, where K is a set from the edges $(\mathbb{SR}, \mathbb{H})$ or (\mathbb{H}, \mathbb{B}) and C_K its Scott-completion, all fulfill

$$D(K) = r(K) + R(K)$$

too, filling the facet in horizontal lines with respect to the inradius-axis.

Hence (*ib*₂) induces the fourth linear facet. Its boundary edges are $(\mathbb{SR}, \mathbb{H})$ (general hoods), (\mathbb{H}, \mathbb{B}) (rounded hoods), $(\mathbb{SR}, \mathbb{RT})$ (concentric sliced Reuleaux triangles), and $(\mathbb{RT}, \mathbb{B})$ (rounded Reuleaux triangles).

(*ib*₃) As shown in [14] a set $K \in \mathcal{K}^2$ fulfills

$$D(K) = \sqrt{3}R(K),$$

iff K contains an equilateral triangle $\mathbb{I}_{\pi/3}$ of the same circumradius. Since \mathbb{RT} is the unique Scott-completion of $\mathbb{I}_{\pi/3}$, we obtain $\mathbb{I}_{\pi/3} \subset K \subset \mathbb{RT}$.

Consider a Reuleaux blossom $\text{RB}_r = 2r\mathbb{I}_{\pi/3} \cap \mathbb{RT}$ with $r \in [r(\mathbb{I}_{\pi/3}), r(\mathbb{RT})]$. We describe a continuous transformation of RB_r , keeping its inradius, diameter, and circumradius constant and decreasing its width until it becomes a set from the edge $(\mathbb{I}_{\pi/3}, \mathbb{FR})$ or $(\mathbb{FR}, \mathbb{SR})$. Let p^i , $i = 1, 2, 3$, s. t. $\mathbb{I}_{\pi/3} = \text{conv}\{p^1, p^2, p^3\}$. While the transformation ending in the sets from the edge $(\mathbb{I}_{\pi/3}, \mathbb{FR})$ can be done within one

step (Step (i) below) the transformation of the sets which should approach the edge $(\mathbb{FR}, \mathbb{SR})$ must be done in two steps (Step (i) and (ii) below):

- (i) We translate $2r\mathbb{I}_{\pi/3}$ in direction of p^1 , until either its inball becomes tangent to $[p^2, p^3]$ (when $r(\mathbb{I}_{\pi/3}) \leq r \leq r(\mathbb{FR})$) or tangent to both arcs of \mathbb{RT} intersecting in p^1 (when $r(\mathbb{FR}) \leq r \leq r(\mathbb{SR})$, see Figure 13.1). We define the *(non-concentric) Reuleaux blossom* by $\mathbb{RB}_{r,v} = (v + 2r\mathbb{I}_{\pi/3}) \cap \mathbb{RT}$, where v is a point on the segment $[0, tp^1]$ with $0 \leq t < 1$ chosen, s. t. in case of $v = tp^1$ one of the two stopping reasons for the translation is reached (cf. Figure 13.1).

Observe that when $r(\mathbb{I}_{\pi/3}) \leq r \leq r(\mathbb{FR})$ all radii of \mathbb{RB}_{r,tp^1} coincide with the ones of a bent equilateral $\mathbb{BI}_{r,\pi/3}$ (cf. Figure 9), which means that we finished the transformation.

- (ii) In case of $r(\mathbb{FR}) \leq r \leq r(\mathbb{SR})$ we further need to reduce the width. However, since the tangent lines to the inball do not support the diameter arcs of \mathbb{RT} intersecting in p^1 , we first “fill” the space between \mathbb{RB}_{r,tp^1} and these arcs, keeping all radii constant, but obtaining a maximal set. Afterwards let L be a line containing p^2 and cutting the extreme Reuleaux blossom \mathbb{RB}_{r,tp^1} , s. t. the distance of p^1 and L is the same as the width of \mathbb{RB}_{r,tp^1} . Then we rotate L continuously until it becomes tangent to the inball of \mathbb{RB}_{r,tp^1} (see Figure 13.2). Denoting the halfspace induced by L containing the inball L^- , we define the *general sliced Reuleaux triangle* as $\mathbb{SR}_{r,w} = \mathbb{RB}_{r,tp^1} \cap L^-$. Finally, when L^- becomes tangent to the inball, we need to “fill” again, this time all the space of \mathbb{RT} inside L^- . Observe that in that moment the general sliced Reuleaux triangle reaches the edge $(\mathbb{FR}, \mathbb{SR})$ becoming a maximally sliced Reuleaux triangle and that starting with the Reuleaux triangle the general sliced Reuleaux triangles get concentric ones and approach \mathbb{SR} .

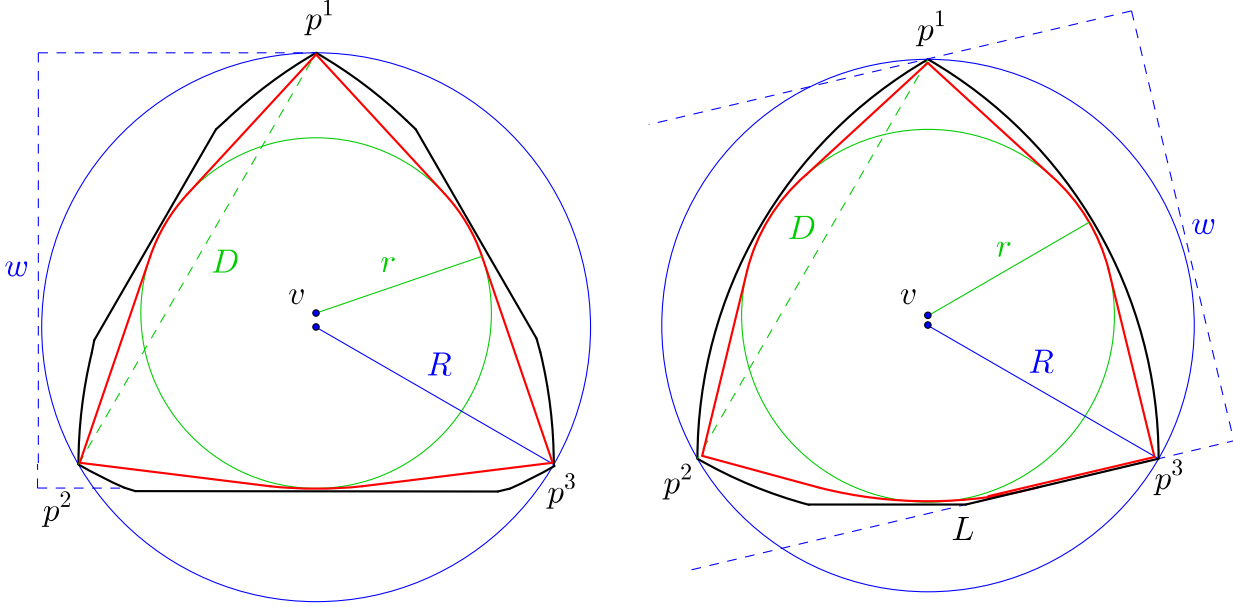
Observe that in that moment the general sliced Reuleaux triangle reaches the edge $(\mathbb{FR}, \mathbb{SR})$ becoming a maximally sliced Reuleaux triangle and that starting with the Reuleaux triangle the general sliced Reuleaux triangles get concentric ones and approach \mathbb{SR} .

Both, non-concentric Reuleaux blossoms and general sliced Reuleaux triangles are maximal sets with respect to set inclusion. The *corresponding* minimal sets are the convex hull of $\text{conv}(\mathbb{I}_{\pi/3}, v + r\mathbb{B})$ with the intersection of the three balls with radius $w(\mathbb{RB}_{r,v})$ or $w(\mathbb{SR}_{r,w})$, depending if we are in case (i) or (ii), around the vertices of $\mathbb{I}_{\pi/3}$.

- (lb₂) It was shown in [13] that every isosceles \mathbb{I}_γ , $\gamma \in [0, \pi/3]$, fulfills

$$(4R(K)^2 - D(K)^2)D(K)^4 = 4w(K)^2R(K)^4$$

with equality. But as already described in [4] they are not the only ones. Since r does not appear in this inequality any superset of an isosceles \mathbb{I}_γ keeping the same circumradius, diameter, and width is mapped to the same facet. This is true, e. g. for all bent trapezoids \mathbb{BT}_γ on the edges $[\mathbb{L}, \mathbb{BT}]$ and $[\mathbb{BT}, \mathbb{FR}]$ and surely also for any minimal version $\text{conv}(\mathbb{I}_\gamma, c_\gamma + r(\mathbb{BT}_\gamma)\mathbb{B})$, where c_γ denotes an incenter of \mathbb{BT}_γ . Thus choosing any $r \in [r(\mathbb{I}_\gamma), r(\mathbb{BT}_\gamma)]$ and an appropriate incenter c (which in many cases will not be unique, as the centers c_γ of \mathbb{BT}_γ where not always unique) the sets $\text{conv}(\mathbb{I}_\gamma, c + r\mathbb{B})$ would have inradius r and the same circumradius, diameter, and width than \mathbb{I}_γ and \mathbb{BT}_γ (see Figure 14). Hence the facet induced by (lb₂) is filled by those sets and bounded by the edges $(\mathbb{L}, \mathbb{I}_{\pi/3})$ (isosceles triangles with $\gamma \in [0, \pi/3]$), $(\mathbb{L}, \mathbb{BT})$, and $(\mathbb{BT}, \mathbb{FR})$ (both kinds of bent trapezoids), as well as $(\mathbb{I}_{\pi/3}, \mathbb{FR})$ (bent equilaterals with the inball being tangent to an edge of $\mathbb{I}_{\pi/3}$).



13.1: In black a non concentric Reuleaux blossom and in red the corresponding minimal set.

13.2: In black a sliced Reuleaux triangle and the corresponding minimal set in red.

FIGURE 13. Examples for the sets, which are mapped onto (ib_3) , corresponding to the cases (i) and (ii) in the description.

Finally, one should recognize that for any fixed center c the sets $\text{conv}(\mathbb{I}_\gamma, c + r\mathbb{B})$ are minimal sets with respect to set inclusion mapped to these coordinates in the diagram and are constructed in the same way than the bent isosceles in (lb_3) below.

- (lb_3) For any $r \in [0, 1]$ and $\gamma \in [0, \pi/3]$ let
- (i) $p^1, p^2, p^3 \in \mathbb{S}$, s. t. $\mathbb{I}_\gamma = \text{conv}\{p^1, p^2, p^3\}$ with $D(\mathbb{I}_\gamma) = \|p^1 - p^2\| = \|p^1 - p^3\|$,
 - (ii) $c \in \mathbb{R}^2$, s. t. the ball $c + r\mathbb{B}$ is tangent to the two arcs with centers p^1, p^2 and radius $D(\mathbb{I}_\gamma)$,
 - (iii) L_1 be the one of the two lines containing p^2 and supporting $c + r\mathbb{B}$ having the smaller angle with $[p^1, p^2]$ and
 - (iv) L_2 be the parallel line of L_1 passing through p^3 .

Then a *generalized bent pentagon* $\text{BP}_{r,\gamma}$ is defined as the space contained between L_1, L_2 and the arcs of radius $D(\mathbb{I}_\gamma)$ around the centers p^1, p^2 , and p^3 (see Figure 15).

If we can ensure that $\mathbb{I}_\gamma \subset \text{BP}_{r,\gamma}$, that $c + r\mathbb{B}$ is the inball of $\text{BP}_{r,\gamma}$, and that $w(\text{BP}_{r,\gamma}) = d(L_1, L_2)$, we simply call it a *bent pentagon* (see Figure 15.1).

Recall the following edges: the bent trapezoids from $(\mathbb{BT}, \mathbb{FR})$, the bent pentagons from $(\mathbb{BT}, \mathbb{H})$, the maximally-sliced Reuleaux triangles from $(\mathbb{FR}, \mathbb{SR})$, and the general hoods from $(\mathbb{SR}, \mathbb{H})$. It is easy to check from their construction that they all are particular cases of bent pentagons in the above sense. We will justify why they describe the boundaries of (lb_3) in showing that they bound the range of the parameters r, γ , s. t. a generalized bent pentagon is a bent pentagon (the bent pentagons and the bent trapezoids bound γ from below while the general hoods and the maximally-sliced Reuleaux triangles bound γ from above).

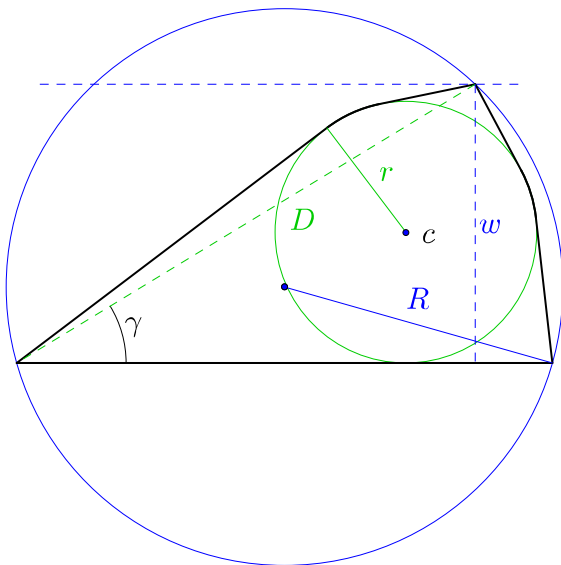
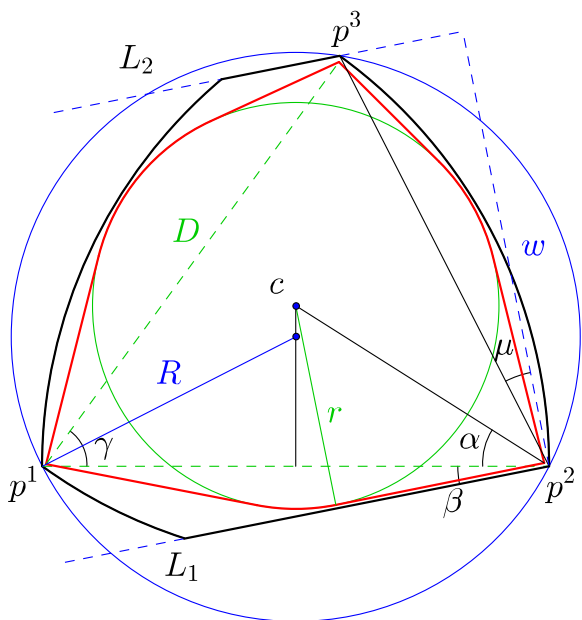
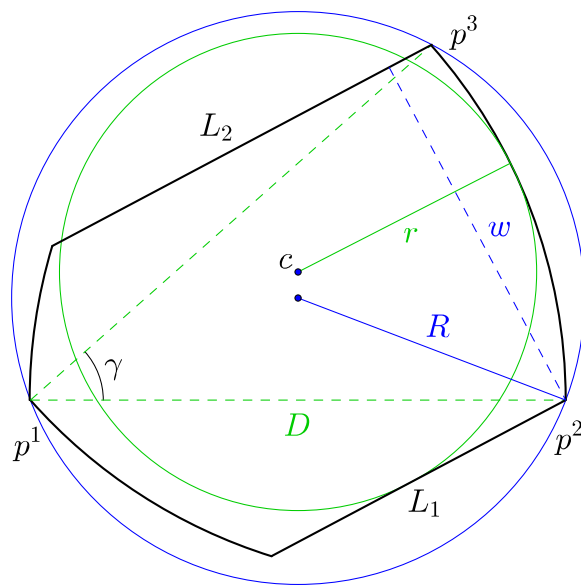


FIGURE 14. An example of a minimal set from (lb_2) .



15.1: A bent pentagon $BP_{r,\gamma}$ (black) and a bent isosceles $BI_{r,\gamma}$ (red), the maximal and minimal sets mapped to the same coordinates in (lb_3) .



15.2: A generalized bent pentagon not being a bent pentagon as $r(BP_{r,\gamma}) < r$.

FIGURE 15. Generalized bent pentagons

Lemma 4.2. *Let $r \in [0, 1]$, $\gamma, \bar{\gamma} \in [0, \pi/3]$ with $\gamma < \bar{\gamma}$, as well as L_1, L_2 and \bar{L}_1, \bar{L}_2 the corresponding parallels in the construction of the generalized bent pentagon $\text{BP}_{r,\gamma}$ and $\text{BP}_{r,\bar{\gamma}}$, respectively. Then*

- a) *the ball $c + r\mathbb{B}$ used in the construction intersects (is tangent to) $[p^1, p^2]$, iff $8r \geq 3D(\text{I}_\gamma)$ ($8r = 3D(\text{I}_\gamma)$).*
- b) *if we restrict to the case $8r \geq 3D(\text{I}_\gamma)$, then it holds $d(L_1, L_2) < d(\bar{L}_1, \bar{L}_2)$.*

Proof. a) The distance from c to $[p^1, p^2]$ is at most r , iff $[p^1, p^2]$ intersects $c + r\mathbb{B}$, that is, when $d(c, [p^1, p^2])^2 = (D(\text{BP}_{r,\gamma}) - r)^2 - 1/4 D(\text{BP}_{r,\gamma})^2 \leq r^2$ (cf. the right-angled triangle $T = \text{conv}\{c, p^2, 1/2(p^1 + p^2)\}$ in Figure 15.1). From simplifying we obtain that this is equivalent to $3/4 D(\text{BP}_{r,\gamma}) - 2r \leq 0$ or $8r \geq 3D(\text{BP}_{r,\gamma})$ with equality, iff $r = d(c, [p^1, p^2])$, which means that the inball is tangent to $[p^1, p^2]$.

b) We use the complete notation as in the construction of the bent pentagons, with a bar on top for $\text{BP}_{r,\bar{\gamma}}$ and assume that $[p^1, p^2]$ as well as $[\bar{p}^1, \bar{p}^2]$ are horizontal, below 0 with $p_1^1 \leq p_1^2$ and $\bar{p}_1^1 \leq \bar{p}_1^2$. Then, it follows from Part (a) that all lines $L_i, \bar{L}_i, i = 1, 2$, have non-negative slope. Since the function $f(x) = (x-r)^2 - 1/4 x^2$ is increasing, if $x \geq 2r$ it follows

$$\begin{aligned} d(c, [p^1, p^2]) &= \sqrt{(D(\text{BP}_{r,\gamma}) - r(\text{BP}_{r,\gamma}))^2 - 1/4 D(\text{BP}_{r,\gamma})^2} \\ &> \sqrt{(D(\text{BP}_{r,\bar{\gamma}}) - r(\text{BP}_{r,\bar{\gamma}}))^2 - 1/4 D(\text{BP}_{r,\bar{\gamma}})^2} = d(\bar{c}, [\bar{p}^1, \bar{p}^2]). \end{aligned}$$

Using again the triangle T defined above and the pythagorean theorem, we obtain

$$p_2^2 = -\sqrt{1 - 1/4 D(\text{BP}_{r,\gamma})^2} > -\sqrt{1 - 1/4 D(\text{BP}_{r,\bar{\gamma}})^2} = \bar{p}_2^2.$$

Moreover, since $\gamma < \bar{\gamma}$, rotating I_γ around \mathbb{S} until p^1 becomes \bar{p}^1 , it follows $p^j, j = 2, 3$ belong to the smaller of the two arcs of \mathbb{S} with endpoints $\bar{p}^j, j = 2, 3$ and thus in particular it holds $p_2^3 < \bar{p}_2^3$ after the rotation. Undoing the rotation, i. e. p^1 moves upward and p^2, p^3 downwards into their old positions, it still holds $p_2^3 < \bar{p}_2^3$ and thus also both points p^2, p^3 still lie in the shorter arc of \mathbb{S} with endpoints $\bar{p}^j, j = 2, 3$. Now, it follows from $\gamma < \bar{\gamma}$ that $\|p^1 - p^2\| > \|\bar{p}^1 - \bar{p}^2\|$, which together with $d(c, [p^1, p^2]) > d(\bar{c}, [\bar{p}^1, \bar{p}^2])$ means that the slope of L_1 is less than the one of \bar{L}_1 . Using this fact, we see that if one rotates $\bar{L}_i, i = 1, 2$, around $\bar{p}^i, i = 2, 3$, s. t. they become parallel to $L_i, i = 1, 2$, their distance decreases, but is still bigger than the distance between L_1 and L_2 . Hence $w(\text{BP}_{r,\gamma}) = d(L_1, L_2) < d(\bar{L}_1, \bar{L}_2) = w(\text{BP}_{r,\bar{\gamma}})$. □

Hence we see that only if Part (a) of Lemma 4.2 holds (which is, because of $D(\text{I}_\gamma) = 2R(\text{I}_\gamma) \cos(\gamma/2)$, equivalent to $\gamma \geq 2 \arccos(4/3r)$), we have $\text{I}_\gamma \subset \text{BP}_{r,\gamma}$, the latter implying that $R(\text{BP}_{r,\gamma}) = R(\text{I}_\gamma)$ and $D(\text{BP}_{r,\gamma}) = D(\text{I}_\gamma)$.

Now considering $c + r\mathbb{B}$, we show that it is the inball of $\text{BP}_{r,\gamma}$ (which means that $r(\text{BP}_{r,\gamma}) = r$), whenever r, γ are in the range described by the edges above. To do so, it is enough to show that L_2 does not intersect the interior of $c + r\mathbb{B}$. However, using Part (b) of Lemma 4.2, it follows that if r, γ determine a bent pentagon with maximal γ depending on r (i. e. $\text{BP}_{r,\gamma}$ belongs to (FR, SR) or (SR, HI)) then L_2 does not intersect $c + r\mathbb{B}$. Decreasing γ decreases monotonously $d(L_1, L_2)$ until $\text{BP}_{r,\gamma}$ becomes a set from (BT, FR) or (BT, HI) and in both cases L_2 does not intersect $c + r\mathbb{B}$ at any point of the transformation (except for the sets in (BT, HI) , where it becomes tangent).

Finally, from Part (b) of Proposition 1.1, we know that the width of $\text{BP}_{r,\gamma}$ must be attained between two supporting parallel lines touching the endpoints of a perpendicular segment in $\text{BP}_{r,\gamma}$. However, considering the construction of the generalized bent pentagons, any such pair of parallel supporting lines, except L_1, L_2 , touches an arc of $\text{BP}_{r,\gamma}$ and the vertex it is drawn around, therefore having a distance of $D(\text{BP}_{r,\gamma}) \geq d(L_1, L_2)$ (cf. Figure 15.1). (Observe that this argument fails if the pentagon does not fulfill Part (a) of Lemma 4.2, as p^1 would not belong to $\text{BP}_{r,\gamma}$ anymore.) Hence $w(\text{BP}_{r,\gamma}) = d(L_1, L_2)$.

The given boundaries for the bent pentagons are best possible. Considering the upper bounds first, on the one hand $\gamma \leq \pi/3$ by definition and for all $r \in [r(\mathbb{FR}), r(\mathbb{SR})]$ this bound is reached by a maximally-sliced Reuleaux triangle $\text{SR}_{r,w_r} = \text{BP}_{r,\pi/3}$.

On the other hand, in case of $r \in [r(\mathbb{SR}), r(\mathbb{H})]$, inequality (ib₂) implies that $D(\text{BP}_{r,\gamma}) \geq r + R(\text{BP}_{r,\gamma}) = D(\text{BP}_{r,2\arccos((r+1)/2)})$, which together with $D(\text{BP}_{r,\gamma}) = D(\text{I}_\gamma) = 2R(\text{I}_\gamma) \cos(\gamma/2)$ and $D(\text{I}_\gamma)$ descending as a function of γ , implies that $\gamma \leq 2\arccos((r+1)/2)$. Equality in this situation is attained by the general hoods.

Regarding the lower bounds, in both cases choosing γ below the given bound yields a generalized bent pentagon not being a bent pentagon: As already mentioned, Part (a) of Lemma 4.2 implies $\gamma \geq 2\arccos(4/3r)$ in general. And in case of $r \in [r(\mathbb{BT}), r(\mathbb{H})]$ choosing $2\arccos(4/3r) \leq \gamma < \bar{\gamma} = \gamma_r$, Part (b) of Lemma 4.2 says that $d(L_1, L_2) < d(\bar{L}_1, \bar{L}_2)$. But since L_1 supports $c + r\mathbb{B}$ and both $\bar{L}_i, i = 1, 2$ support the inball of BP_{r,γ_r} , it follows that L_2 would intersect the interior of $c + r\mathbb{B}$.

For the computation of the radii we denote the angle in p^2 between $[p^1, p^2]$ and $[c, p^2]$ by α , the angle in p^2 between $[p^1, p^2]$ and L_1 by β , as well as the angle in p^2 between $[p^2, p^3]$ and the line perpendicular to L_1 by $\mu = \gamma/2 - \beta$ (cf. Figure 15.1). Omitting again the argument $\text{BP}_{r,\gamma}$ in the radii functionals, it holds

$$(i) \cos(\alpha) = \frac{D}{2(D-r)}, \quad (ii) \sin(\alpha + \beta) = \frac{r}{D-r}, \quad (iii) \cos(\mu) = \frac{w}{\|p^2 - p^3\|}.$$

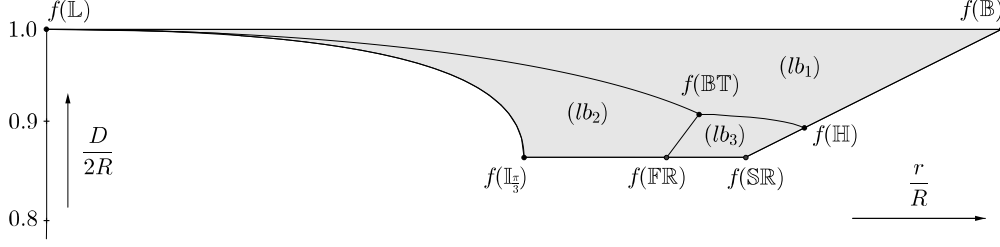
From (i) and (ii) we obtain that $\beta = \arcsin(r/D-r) - \arccos(D/2(D-r))$, which together with $\gamma = 2\arccos(D/2R)$ implies $\mu = \frac{\gamma}{2} - \beta = \arccos(D/2R) + \arccos(D/2(D-r)) - \arcsin(r/D-r)$. Inserting μ and $\|p^2 - p^3\| = 2D\sqrt{1 - (D/2R)^2}$ into (iii) results in

$$(7) \quad w = 2D\sqrt{1 - (D/2R)^2} \cos\left(\arccos\left(\frac{D}{2(D-r)}\right) + \arccos\left(\frac{D}{2R}\right) - \arcsin\left(\frac{r}{D-r}\right)\right).$$

Thus each $\text{BP}_{r,\gamma}$ satisfies (lb₃) with equality.

Again, we also define the bent isosceles $\text{BI}_{r,\gamma} := \text{conv}(\text{I}_\gamma, c + r\mathbb{B})$, which obviously fulfill $R(\text{BI}_{r,\gamma}) = R(\text{BP}_{r,\gamma})$, $D(\text{BI}_{r,\gamma}) = D(\text{BP}_{r,\gamma})$, and $r(\text{BI}_{r,\gamma}) = r(\text{BP}_{r,\gamma})$. Using Lemma 4.2, we know that $c + r\mathbb{B}$ intersects all three edges of I_γ . However, from Part (b) of Proposition 1.1 it follows, that the width of $\text{BI}_{r,\gamma}$ is necessarily attained between a parallel pair of lines, from which one supports the inball and a vertex and the other a different vertex. Doing a direct comparison among the six pairs of such parallel supporting lines, we easily obtain $w(\text{BI}_{r,\gamma}) = d(L_1, L_2) = w(\text{BP}_{r,\gamma})$ (cf. Figure 15.1). Hence it holds $f(K) = f(\text{BP}_{r,\gamma})$, iff $\text{BI}_{r,\gamma} \subset K \subset \text{BP}_{r,\gamma}$.

(ub₂) Let $\gamma \in [\pi/3, \pi/2]$, $r \in [r(\text{I}_\gamma), r(\text{SB}_\gamma^\circ)]$, and p^1, p^2, p^3 , s. t. $\text{conv}\{p^1, p^2, p^3\} = \text{I}_\gamma$. Then $I_K = \frac{r}{r(\text{I}_\gamma)}(\text{I}_\gamma - p^3) + p^3 = \text{conv}\{q^1, q^2, p^3\}$ is an isosceles triangle of inradius r , s. t. $q^i = \frac{r}{r(\text{I}_\gamma)}p^i + (1 - \frac{r}{r(\text{I}_\gamma)})p^3$, $i = 1, 2$ (cf. Figure 17.1). We call the sets $\text{SB}_{r,\gamma} =$

FIGURE 16. Bottom view of the diagram $f(\mathcal{K}^2)$.

$I_K \cap \mathbb{B}$ (*general sailing boats*), generalizing the concentric and right-angled sailing boats which are mapped to the edges $(\mathbb{I}_{\pi/3}, \mathbb{I}_{\pi/2})$ and $(\mathbb{I}_{\pi/3}, \mathbb{SB})$.

It follows directly from the definition that $p^1 \in [q^1, p^3] \cap \mathbb{S}$ and $p^2 \in [q^2, p^3] \cap \mathbb{S}$ and thus $R(\text{SB}_{r,\gamma}) = R(\mathbb{I}_\gamma)$, $D(\text{SB}_{r,\gamma}) = D(\mathbb{I}_\gamma) = 2R(\text{SB}_{r,\gamma}) \sin(\gamma)$ and $r(\text{SB}_{r,\gamma}) = r(I_K) = r$. Moreover, since $\mathbb{I}_\gamma \subset \text{SB}_{r,\gamma} \subset \text{SB}_\gamma^\circ$, the width of $\text{SB}_{r,\gamma}$ is obviously taken between $[q^1, q^2]$ and p^3 , s. t.

$$w(\text{SB}_{r,\gamma}) = r \frac{w(\mathbb{I}_\gamma)}{r(\mathbb{I}_\gamma)} = r \left(1 + \frac{1}{\sin(\gamma/2)} \right) = r \left(1 + \frac{2\sqrt{2}R}{D} \sqrt{1 + \sqrt{1 - \left(\frac{D}{2R}\right)^2}} \right).$$

Thus all general sailing boats $\text{SB}_{r,\gamma}$ are extreme for the inequality (*ub*₂).

Since $\text{SB}_{r(\mathbb{I}_\gamma),\gamma} = \mathbb{I}_\gamma$, $\text{SB}_{r(\text{SB}_\gamma^\circ),\gamma} = \text{SB}_\gamma^\circ$, and $\text{SB}_{r,\pi/2}$ a right-angled sailing-boat, the edges $(\mathbb{I}_{\pi/3}, \mathbb{I}_{\pi/2})$, $(\mathbb{I}_{\pi/3}, \mathbb{SB})$, and $(\mathbb{I}_{\pi/2}, \mathbb{SB})$ form the boundaries of this facet.

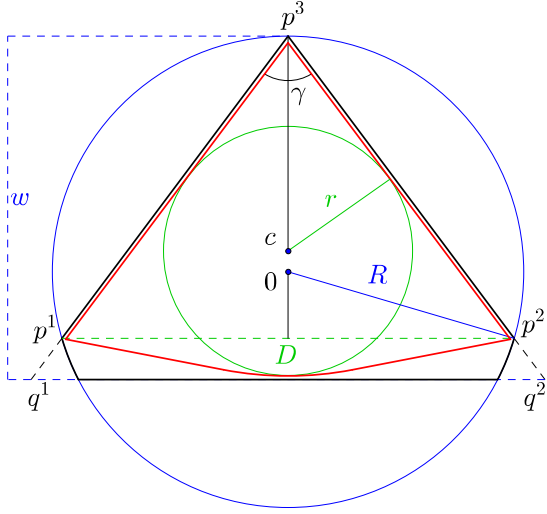
While it holds $K \subset \text{SB}_{r,\gamma}$ for all set K with $f(K) = f(\text{SB}_{r,\gamma})$, in general there do not exist unique minimal sets, as we have already discussed for the edge $(\mathbb{I}_{\pi/2}, \text{SB}_{r,\pi/2})$. However, if $w(\text{SB}_{r,\gamma}) \leq \|p^1 - p^3\|$, the minimal set $\text{conv}(\mathbb{I}_\gamma, (p^3 + w(\text{SB}_{r,\gamma})\mathbb{B}) \cap \text{SB}_{r,\gamma})$ is unique (cf. Figure 17.1).

(*ub*₃) Any *acute triangle* is circumspherical, i. e. all its vertices are situated on the circum-sphere. For any $D \in [\sqrt{3}/2, 1]$ consider the two angles $0 \leq \gamma_1 \leq \pi/3 \leq \gamma_2 \leq \pi/2$, s. t. $D(\mathbb{I}_{\gamma_1}) = D(\mathbb{I}_{\gamma_2}) = D$. It is easy to see that for any $r \in [r(\mathbb{I}_{\gamma_1}), r(\mathbb{I}_{\gamma_2})]$ there exists an acute triangle $\text{T}_{r,D}$ with the same circumradius and diameter as \mathbb{I}_{γ_1} and \mathbb{I}_{γ_2} and inradius r .

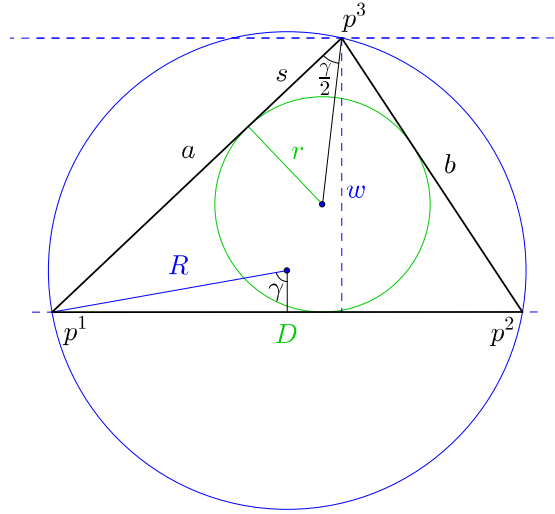
Since every acute triangle is enclosed (in the above sense) between two isosceles triangles with the same diameter and circumradius, the edges $(\mathbb{L}, \mathbb{I}_{\pi/3})$, $(\mathbb{I}_{\pi/3}, \mathbb{I}_{\pi/2})$ (both kinds of isosceles triangles) and the edge $(\mathbb{L}, \mathbb{I}_{\pi/2})$ (right-angled triangles) form the relative boundary of this facet.

Let γ denote the angle of $\text{T}_{r,D}$ at the vertex p^3 , opposing the diametral edge $[p^1, p^2]$ and s the distance within the other two edges of p^3 to the touching points of the inball (see Figure 17.2). Then, as we have used already in the computations of the edge $(\mathbb{L}, \mathbb{I}_{\pi/2})$ in 4.2, the perimeter of $\text{T}_{r,D}$ is $2(s + D)$. Thus using the semiperimeter formula for the area of a triangle, Proposition 1.3 and simple trigonometry, we get

$$(i) \ wD = 2r(s + D), \quad (ii) \ D = 2R \sin(\gamma) \quad (iii) \ r = s \tan(\gamma/2),$$



17.1: A general sailing boat $SB_{r,\gamma}$ in black, and a corresponding minimal set in red.



17.2: An acute triangle $T_{r,D}$.

FIGURE 17. The general sailing boats and acute triangles fill the two remaining facets of the upper boundary.

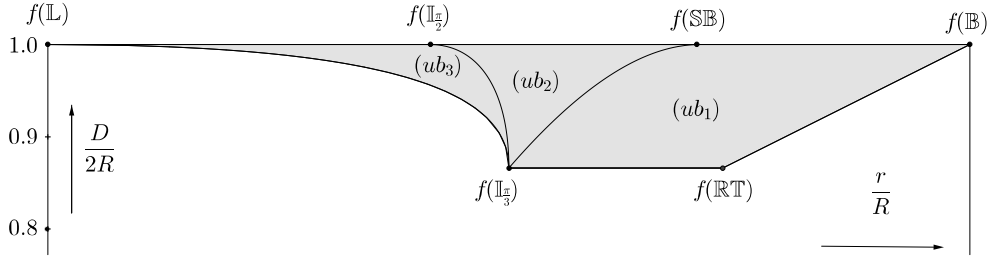


FIGURE 18. Top view of the diagram $f(K^2)$.

(cf. Figure 17.2). Now, substituting the value of s in (i) by $s = \frac{r}{\tan(\gamma/2)}$ obtained from (iii), while using (ii) to replace γ , we finally arrive in

$$wD = 2r \left(D + \frac{r}{\tan\left(\frac{1}{2} \arcsin\left(\frac{D}{2R}\right)\right)} \right) = 2r \left(D + \frac{2rR}{D} \left(1 + \sqrt{1 - \left(\frac{D}{2R}\right)^2} \right) \right).$$

5. PROOFS OF THE MAIN RESULTS

In this section we give the proofs of the main theorems. For preparation, we first state a corollary and some technical lemmas.

Corollary 5.1. *Let $K \in \mathcal{K}^n$ and $c \in \mathbb{R}^n$, s. t. $c + \rho\mathbb{B} \subset K \subset \mathbb{B}$, $p^1, \dots, p^k, u^1, \dots, u^l$ as in Proposition 1.2, $T = c + \bigcap_{i=1}^l \{x \in \mathbb{R}^n : (u^i)^T x \leq \rho\}$ and $T' = \text{conv}\{p^1, \dots, p^k\}$. Then*

- a) at least two of the vertices of T do not belong to $\text{int}(\mathbb{B})$, and
 b) T' separates $\text{bd}(T)$ from 0 .

Proof. Both statements follow directly from $0 \in T' \subset K \subset T$, recognizing that, if all but at most one vertex of T would belong to $\text{int}(\mathbb{B})$, it would follow that $R(K) < 1$, a contradiction. \square

While Proposition 1.2 in Section 1 deduces properties of the inner and outer radii separately from their definitions, Corollary 5.1 already combines them. In the following lemmas, we derive some properties from the interaction between both of them and the diameter.

We recall that we always assume \mathbb{B} to be the circumball of K even though keeping the value $R(K)$ in the equations.

Lemma 5.2. *Let $K \in \mathcal{K}^n$ and $c \in \mathbb{R}^n$, s. t. $c + r(K)\mathbb{B} \subset K \subset \mathbb{B}$. Then there exist u^1, \dots, u^l and T as in Corollary 5.1, as well as $u \in \mathbb{S}$ s. t. $\mathbb{S}_u^{\geq} \subset T \cap \mathbb{S}$ and $\mathbb{S}_u^{\geq} \cap \text{bd}(T) = \emptyset$, iff $K = \mathbb{B}$, $r(K) = 1$ and $c = 0$.*

Proof. For the “if”-direction, we easily see that if $K = \mathbb{B}$ then choosing $l = 2$ and $u^2 = -u^1$ and any u orthogonal to u^1 , we obtain $T \cap \mathbb{S} = \mathbb{S} \supset \mathbb{S}_u^{\geq}$ and $\mathbb{S}_u^{\geq} \cap \text{bd}(T) = \emptyset$.

For proving the “only if”-direction let us assume $r(K) < 1$. Then, however u^1, \dots, u^l and u are chosen, they must satisfy $0 \in \text{conv}\{u^1, \dots, u^l\}$ and thus there exists $j \in [l]$, s. t. $u^T u^j \geq 0$ and $u^j \in \mathbb{S}_u^{\geq}$.

Since $c + r(K)\mathbb{B} \subset \mathbb{B}$, it holds $\|c\| + r(K) \leq 1$ and therefore $c^T u^j + r(K) \leq \|c\| \|u^j\| + r(K) = \|c\| + r(K) \leq 1$, which, as $u^j \in \mathbb{S}$, implies $(u^j - c)u^j \geq r(K)$ and “=” holds, iff $c = (1 - r(K))u^j$, which means $u^j = c + r(K)u^j$.

Now, in case of $(u^j - c)u^j > r(K)$, it follows $u^j \notin c + \{x \in \mathbb{R}^n : x^T u^j \leq r(K)\} \supset T \supset \mathbb{S}_u^{\geq}$, contradicting $u^j \in \mathbb{S}_u^{\geq}$.

On the other hand, if $(u^j - c)u^j = r(K)$, it holds $u^j = c + r(K)u^j \in c + \{x \in K : x^T u^j = r(K)\} \subset \text{bd}(T)$. However, since $\mathbb{S}_u^{\geq} \cap \text{bd}(T) = \emptyset$, it follows $u^j \in \mathbb{S}_u^{\geq} \setminus \mathbb{S}_u^{\geq} = \mathbb{S} \cap \{x : u^T x = 0\}$ and therefore $u^T u^j = 0$. Now, since $0 \in \text{conv}\{u^1, \dots, u^l\}$, there exists $k \in [l] \setminus \{j\}$, s. t. $u^T u^k \geq 0$. But, since $c + r(K)u^k \in \mathbb{S}$ would mean that there exist two different points of $c + r(K)\mathbb{B}$ in \mathbb{S} , contradicting $r(K) < 1$, we must have $c + r(K)u^k \notin \mathbb{S}$. Hence $(u^k - c)u^k > r(K)$ as shown above with j instead of k , contradicting $u^k \in \mathbb{S}_u^{\geq}$. \square

Lemma 5.3. *Let $K \in \mathcal{K}^2$ and $c \in \mathbb{R}^2$, s. t. $c + r(K)\mathbb{B} \subset K \subset \mathbb{B}$, as well as p^1, p^2, p^3 (possibly with $p^2 = p^3$), u^1, u^2, u^3 (possibly with $u^2 = u^3$), T , and T' as in Corollary 5.1 for the case $n = 2$. The common supporting lines of K and $c + r(K)\mathbb{B}$ with outer normals u^1, u^2, u^3 are denoted by L_1, L_2, L_3 , respectively, the halfspaces induced by these lines containing K by L_1^-, L_2^-, L_3^- (thus $T' := \text{conv}\{p^1, p^2, p^3\}$ and $T := L_1^- \cap L_2^- \cap L_3^-$). Finally, define $C := T \cap \mathbb{B}$, and $S_i := L_i \cap C$, $i = 1, 2, 3$. Then*

- a) the line segments of T' separate the line segments S_i of T from 0 within \mathbb{B} .
 b) the length of each line segment S_i , $i = 1, 2, 3$, is at most $D(K)$.
 c) the diameter of C is taken between two points on different arcs of $C \cap \mathbb{S}$ or $D(C) = 2$.
 d) there exist $q^1, q^2 \in C \cap \mathbb{S}$ s. t. $\|q^1 - q^2\| = D(K)$ and the segment $[q^1, q^2]$ separates one of the segments S_i , $i = 1, 2, 3$, from the other two segments and the origin 0 (see Figure 19 as an example).

Proof. a) This is a direct interpretation of Part (b) of Corollary 5.1 in \mathbb{R}^2 (but only there).
 b) If the length of S_i would be greater than $D(K)$, the same would be true for the segment of T' separating S_i from 0 , a contradiction as $T' \subset K$.
 c) By Proposition 1.1, there exist extreme points z^1, z^2 of C , s. t. $\|z^1 - z^2\| = D(C)$. Using Part (a) of Corollary 5.1, we distinguish the cases where no or one vertex of T belongs to $\text{int}(\mathbb{B})$.

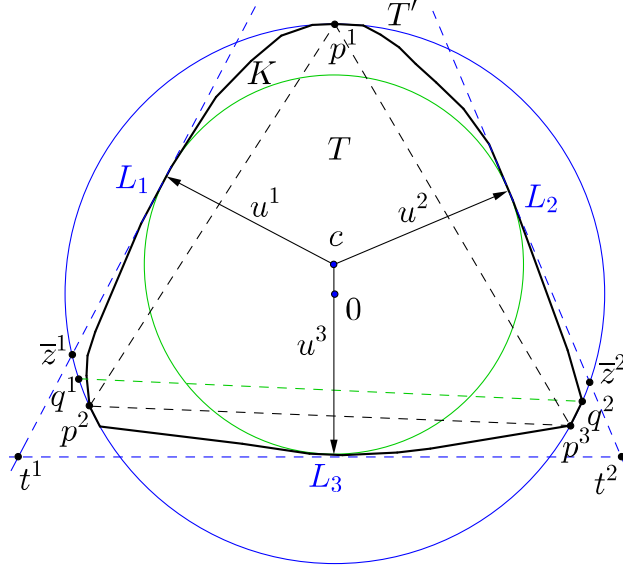


FIGURE 19. A convex set K and all elements of Lemma 5.3. Observe that $q^1 \notin K$.

In the first case, it holds $z^1, z^2 \in \text{ext}(C) = C \cap \mathbb{S}$. We show that if $K \neq \mathbb{B}$, then z^1 and z^2 do not belong to the same arc of $C \cap \mathbb{S}$. If they do, we denote by \bar{z}^i , $i = 1, 2$ the one of the two points in $L_i \cap \mathbb{S}$, which is in the same arc of $C \cap \mathbb{S}$ than z^i (see again Figure 19). (defining that, if a line intersects \mathbb{S} in a single point, then it separates two different arcs).

Using Lemma 5.2, we know that if $K \neq \mathbb{B}$ the arc containing z^1, z^2 is at most an open semisphere. Hence $D(C) = \|z^1 - z^2\| \leq \|\bar{z}^1 - \bar{z}^2\| < 2$ and therefore $\bar{z}^i = z^i$, $i = 1, 2$.

We first consider the case that $L_i \cap \text{int}(\mathbb{B}) \neq \emptyset$, $i = 1, 2$. Since $0 \in \text{conv}\{u^1, u^2, u^3\}$ the lines L_i , $i = 1, 2$ are parallel or intersect in a vertex of T on the same side of 0 than the segment $[z^1, z^2]$.

However, in any of the two cases, the distances between z^1 and any point in $L_2 \cap \text{int}(\mathbb{B})$ or the distance between z^2 and any point in $L_1 \cap \text{int}(\mathbb{B})$ is strictly bigger than $\|z^1 - z^2\| = D(C)$, a contradiction.

Now turn to the case that $L_i \cap \text{int}(\mathbb{B}) = \emptyset$ for at least one $i \in \{1, 2\}$, w.l.o.g. for $i = 1$, which means $\{z^1\} = L_1 \cap \mathbb{S}$ thus L_1 supports \mathbb{B} in z^1 . However, since L_1 supports $c + r(K)\mathbb{B}$ by definition, we obtain that it must support $c + r(K)\mathbb{B}$ in z^1 . Using the fact that the arc containing z^1, z^2 is at most an open semisphere, we have $z^2 \neq -z^1$ and therefore $D(C) \geq D(\text{conv}\{z^2, c + r(K)\mathbb{B}\}) > \|z^1 - z^2\| = D(C)$, again a contradiction.

Finally consider the case that one vertex of T belongs to $\text{int}(\mathbb{B})$. Then $C \cap \mathbb{S}$ contains at most two arcs. Applying Part (a) of Proposition 1.2 for C , there exist p^1, p^2, p^3 in this two arcs, s.t. $0 \in \text{conv}\{p^1, p^2, p^3\}$. However, as two of the p^i have to be on the same arc, the negative of the third has to be on that arc, too, proving $D(C) = 2$ for that case.

d) In case of $K = \mathbb{B}$ the claim is trivially true. Hence we may assume $K \neq \mathbb{B}$.

Using Part (a) of Corollary 5.1, we distinguish again the cases with no or one vertex of T belonging to $\text{int}(\mathbb{B})$.

In the first case, it was shown in Part (c) that any pair of diametral points z^1 and z^2 of C lie in different arcs of $C \cap \mathbb{S}$. But this means that $[z^1, z^2]$ separates one of the segments

S_i from the other two segments and the origin 0, say S_3 (cf. Figure 19). From Part (b) we know that the length of S_3 is at most $D(K) \leq D(C) = \|z^1 - z^2\|$. Hence there exist q^1 and q^2 in the same arcs as z^1 and z^2 , respectively, s. t. $\|q^1 - q^2\| = D(K)$ and $[q^1, q^2]$ still separates S_3 in the same way as $[z^1, z^2]$ does.

If a vertex of T belongs to $\text{int}(\mathbb{B})$, it follows from Part (c) that $D(C) = 2$, which means $z^2 = -z^1$. Thus $[z^1, z^2]$ separates the two segments intersecting in $\text{int}(\mathbb{B})$ from the third. However, again because of Part (b) there must exist q^1 and q^2 with $\|q^1 - q^2\| = D(K)$ separating this third segment from the other two and 0. □

Lemma 5.4. *Consider the same setting and notation as in Lemma 5.3. In the following we assume that the single separated segment in Part (d) of Lemma 5.3 is S_3 and w. l. o. g. that S_3 is horizontal below 0 as well as separated by $[q^1, q^2]$ from S_1, S_2 , and 0. Moreover, we denote the point in C farthest from L_3 by y , the intersection points of $L_i, i = 1, 2$ with L_3 by $t^i, i = 1, 2$, respectively, and assume that $t_1^1 \leq 0 \leq t_1^2$ (which is possible when S_3 is horizontal and means that L_1 bounds S_3 on the left while L_2 bounds S_3 on the right, see Figure 19).*

- a) *The first coordinate of the intersection points of L_1 and \mathbb{S} is bounded from above by $D(K)/2$ while the first coordinate of the intersection points of L_2 and \mathbb{S} is bounded from below by $D(K)/2$.*
- b) *It holds $|y_1| \leq D(K)/2$.*
- c) *One can modify the choice of q^1 and q^2 satisfying Part (d) in Lemma 5.3, s. t. the interior angles of $\text{conv}\{y, q^1, q^2\}$ in q^1 and q^2 are at most $\pi/2$.*

Proof. a) It suffice to show the upper bound in case of L_1 . Since S_3 is the separated segment, it follows $t^1, t^2 \notin \text{int}(\mathbb{B})$ and since S_3 is horizontal, (a) is obviously true for \bar{z}^1 . Now we denote the further one by x^1 and assume $x^1 \geq 0$ as otherwise there is nothing to show. Since S_3 is horizontal, we have $t_1^1 \leq 0$ and $t_2^1 \leq x_2^1$, which means L_1 has a positive slope. Now, assuming $x_1^1 > D(K)/2$ implies together with $\bar{z}_1^1 \leq q_1^1 = -D(K)/2$ that the length of S_1 is strictly greater than $D(K)$, which contradicts Part (c) of Lemma 5.3.

b) Again, it suffices to show $y_1 \leq D(K)/2$, because of symmetry in the argument. If L_1 and L_2 intersect within $\text{int}(\mathbb{B})$, they must intersect in y . Hence $y_1 \leq x_1^1 \leq D(K)/2$ using the notation as in Part (a). Otherwise y lies on the arc of $C \cap \mathbb{S}$ between x^1 and x^2 , its corresponding point in $L_2 \cap \mathbb{S}$. However, with e^2 denoting the second unit vector, that would mean $y \in \{x^1, x^2, e^2\}$, which again proves the claim because of Part (a).

c) We suppose w. l. o. g. that $q^i, i = 1, 2$, belong to the arc of \mathbb{S} induced by S_i and $S_3, i = 1, 2$, respectively. First, it follows from Thales' theorem that the region $R \subset \mathbb{B}$ on the same side as 0 of $[q^1, q^2]$, for which one of the angles would be bigger than $\pi/2$, is the union of the caps of \mathbb{B} induced by $\text{aff}\{q^1, -q^2\}$ and $\text{aff}\{-q^1, q^2\}$, without $\text{aff}\{q^1, -q^2\}$ and $\text{aff}\{-q^1, q^2\}$ themselves.

As we have seen in Part (b), using the notation there and denoting the intersection of L_1 and L_2 by t^3 , it holds $y \in \{x^1, x^2, e^2, t^3\}$. In any of the four cases $[q^1, q^2]$ separates y from S_3 .

Now, we describe the choice of q^1 and q^2 satisfying Part (c) for each of the possible y 's: Since $q_1^1 < 0$ and $q_1^2 > 0$, we obviously have $y \notin R$, if $y = e^2$. To obtain $y = x^i, i = 1, 2$, it must hold that e^2 does not belong to C , which means either $x_1^1 > 0$ and $y = x^1$ or $x_2^1 < 0$ and $y = x^2$. Hence we may assume w. l. o. g. that $y = x^1$ or $y = t^3$ and that, if $y \in R$, then it is contained in the cap induced by $\text{aff}\{-q^1, q^2\}$. Using Part (c) of Lemma 5.3, we know that the length of S_1 is at most $D(K) = \|q^1 - q^2\|$.

Since y is contained in the cap of \mathbb{B} between q^2 and $-q^1$ this is only possible if S_1 cuts through one of the segments $[q^1, q^2]$ or $[-q^2, -q^1]$ (otherwise S_1 would be longer than $\|q^1 - q^2\| = D(K)$, a contradiction). However, the first case would contradict that $[q^1, q^2]$

separates S_1 from S_3 . Hence S_1 must intersect $[-q^2, -q^1]$. Using S_3 being horizontal and therefore S_1 being ascending (and S_2 descending) as well as the fact that $-q^1$ is above y , $[q^1, q^2]$ must be ascending even with a bigger slope than S_1 , since otherwise they could not intersect. But then we may move $q^1, q^2 \in C \cap \mathbb{S}$ inside the same arcs and keeping their distance, until $[q^1, q^2]$ becomes parallel to S_1 , but stays ascending, and therefore not annihilating the separation of S_3 . Rebuilding R from the new vectors q^1, q^2 , we obtain $y \notin R$. □

Before we state the following Lemma, remember that we know from (ub_2) and (ub_3) in Subsection 4.3, that for every diameter $D \in [\sqrt{3}, 2]$ and inradius $r \in [r(\mathbf{I}_{2\arccos(D/2)}), r(\mathbf{SB}_{\arcsin(D/2)}^\circ)]$ there exist triangles $\mathbf{T}_{r,D}$ – in case of $r \leq r(\mathbf{I}_{\arcsin(D/2)})$ – or sailing boats $\mathbf{SB}_{r,\arcsin(D/2)}$ – in case of $r \geq r(\mathbf{I}_{\arcsin(D/2)})$.

Lemma 5.5. *Let $D \in [\sqrt{3}, 2]$ and $r(\mathbf{I}_{2\arccos(D/2)}) \leq r \leq r(\mathbf{SB}_{\arcsin(D/2)}^\circ)$. Then for all $K \in \mathcal{K}^2$, s. t. $D(K) = D$ and $r(K) = r$ there exists*

- a) a triangle $\mathbf{T}_{r,D}$, s. t. $w(K) \leq w(\mathbf{T}_{r,D})$, if $r \leq r(\mathbf{I}_{\arcsin(D/2)})$,
- b) a sailing boat $\mathbf{SB}_{r,\arcsin(D/2)}$, s. t. $w(K) \leq w(\mathbf{SB}_{r,\arcsin(D/2)})$, if $r \geq r(\mathbf{I}_{\arcsin(D/2)})$.

Proof. Let $c \in \mathbb{R}^2$, s. t. $c + r(K)\mathbb{B}$ and \mathbb{B} are the in- and circumball of K , respectively. Using the notation as given in Lemma 5.3, remember that $R(C) = R(K)$ and $r(C) = r(K)$, whereas the monotonicity of the radii with respect to set inclusion implies $D(C) \geq D(K)$ and $w(C) \geq w(K)$.

The idea of the proof is to transform C in several steps into some triangle or sailing boat \bar{C} satisfying $R(\bar{C}) = R(K)$, $r(\bar{C}) = r(K)$, $D(\bar{C}) = D(K)$, and $w(\bar{C}) \geq w(K)$.

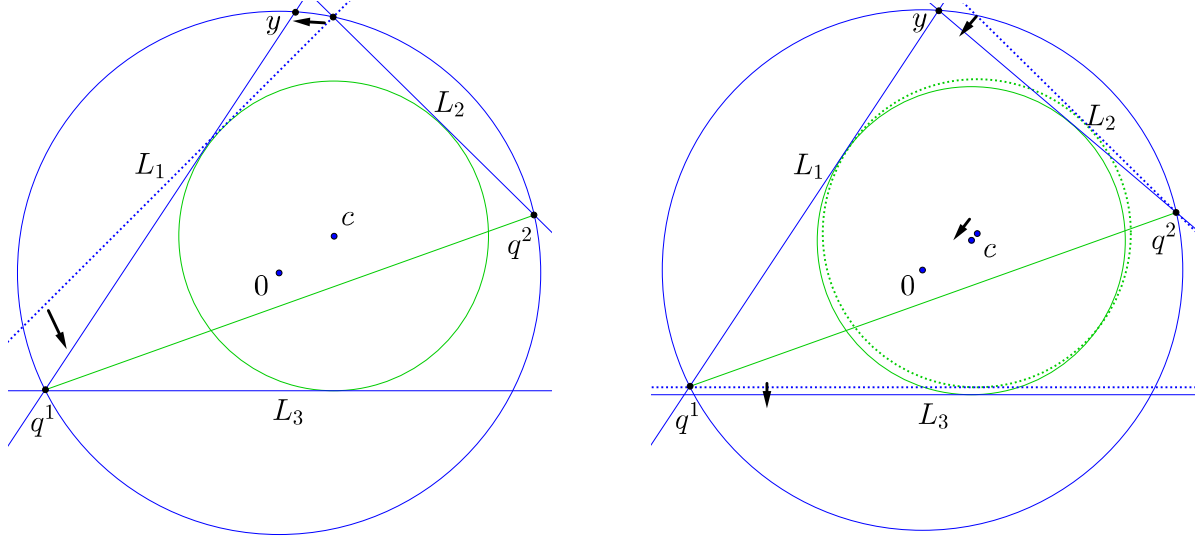
More precisely, denoting the breadth of C in direction of u^3 by $b_{u^3}(C)$, we know from the definitions of the width and the point y in Part (b) of Lemma 5.4, which is the farthest point in C from L_3 , that $w(C) \leq b_{u^3}(C) = \text{dist}(y, L_3)$.

Now, in every step of the transformation of C , we will increase the breadth in direction of u^3 , but arriving in \bar{C} it even holds $w(\bar{C}) = b_{u^3}(\bar{C})$ (as we have seen when defining the triangle and sailing boat families).

- (i) Rotate the lines L_1 and L_2 , s. t. they keep supporting $c + r(K)\mathbb{B}$ and contain q^1 and q^2 , respectively, thus also keeping the separation of S_1, S_2 from S_3 by $[q^1, q^2]$. In the degenerate case of only two supporting parallel hyperplanes to $c + r(K)\mathbb{B}$ (which means by the choices in the proof of Lemma 5.3 that $u^1 = u^2$), we substitute L_1 by two lines L_1 and L_2 supporting $c + r(K)\mathbb{B}$ and containing q^1 and q^2 , respectively, s. t. $0 \in \text{int}(\text{conv}\{u^1, u^2, u^3\})$ and arrive in the same situation then in the non-degenerate case.

Thus, the y we have before the change still belongs to C afterwards and therefore the new y (the point at maximum distance from L_3 within the new C) is not closer to L_3 than before. Applying Parts (b) and (c) of Lemma 5.4 for the new C , we still have that $|y_1| \leq D(K)/2$ and that $\text{conv}\{y, q^1, q^2\}$ has interior angles in q^1 and q^2 at most $\pi/2$.

- (ii) This step is only needed, if $L_1 \cap L_2 \notin \mathbb{B}$, which means that $y \in \{x^1, x^2, e^2\}$. First, as long as $y \notin L_2$ we translate $c + r(K)\mathbb{B}$ downwards, parallel to L_1 , rotate L_2 around the point q^2 and move L_3 parallel to its prior position, s. t. L_2 and L_3 keep supporting $c + r(K)\mathbb{B}$. Afterwards, as long as $y \notin L_1$ we translate $c + r(K)\mathbb{B}$ downwards, parallel to L_2 , rotate L_1 around the point q^1 and move L_3 again parallel to its prior position, s. t. L_1 and L_3 keep supporting $c + r(K)\mathbb{B}$. In the end y is in $L_1 \cap L_2 \cap \mathbb{S}$ and since L_3 moves always vertically downwards, but y stays equal, the distance $\text{dist}(y, L_3)$ does not decrease.
- (iii) Since the inner angles of $\text{conv}\{y, q^1, q^2\}$ in q^1 and q^2 are at most $\pi/2$, the distance of the intersection points t^i , $i = 1, 2$, of L_3 with L_i , $i = 1, 2$, is at least $\|q^1 - q^2\| = D(K)$.



20.1: In (i) the lines L_1, L_2 may be rotated around $c + r\mathbb{B}$.

20.2: In (ii) we may move $c + r\mathbb{B}$ downwards while L_1 (and/or L_2) may be rotated around q^1 (and/or q^2).

FIGURE 20. Examples for (i) and (ii) in Lemma 5.5. Here and in Figures 21 to 23 the start and the end of a movement are indicated by dotted and, respectively, full lines.

Hence there exist $\bar{q}^i \in L_i, i = 1, 2$, s. t. $[\bar{q}^1, \bar{q}^2]$ is parallel to L_3 and $\|\bar{q}^1 - \bar{q}^2\| = D(K)$. We move T until $\bar{q}^i = q^i, i = 1, 2$, (differently to $\bar{q}^i, i = 1, 2$, the q^i 's are not fixed to the construction of T and therefore are not affected by the rotation) and afterwards rotate everything to have L_3 again horizontal (see Figure 21.1).

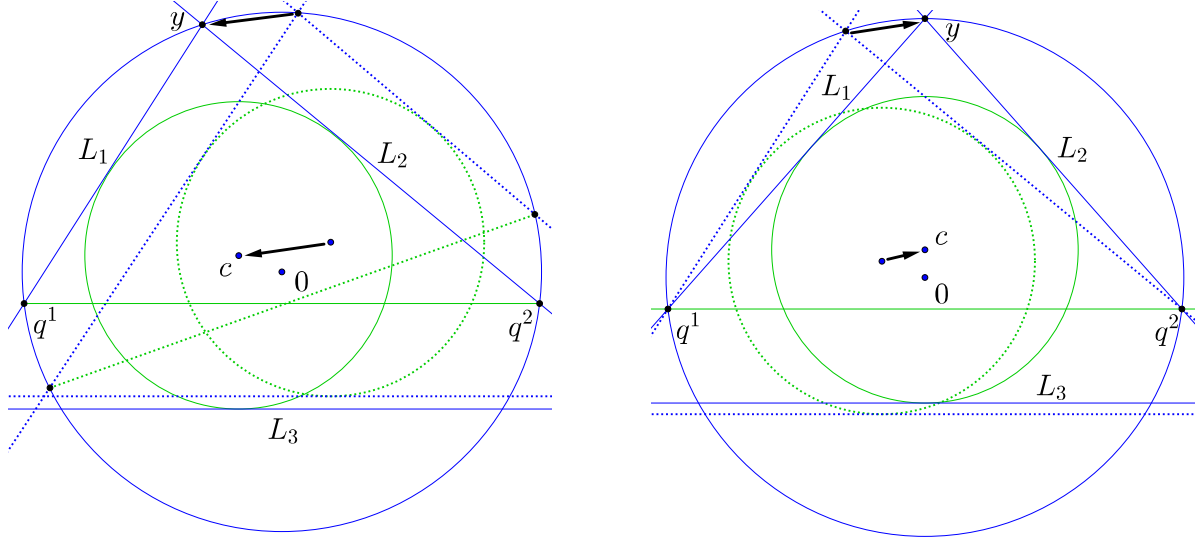
From (ii) it follows $y \in L_1 \cap L_2 \subset \mathbb{B}$ and since T is only moved in (iii) the angle in y of T does not change. Hence Proposition 1.3 with $q^3 = y$ implies that after the movement the vertex y is still in \mathbb{B} , and moreover, if $y \in \mathbb{S}$ before the movement, it will be in \mathbb{S} after, too. Since we just do a solid motion on T , the distance $\text{dist}(y, L_3)$ keeps constant in (iii).

- (iv) If $y \in \mathbb{S}$, we move $\{y\} = L_1 \cap L_2$ around \mathbb{S} towards e^2 and L_1 and L_2 with it. The inball is moved, s. t. it remains tangent to both L_1 and L_2 and the line L_3 parallel to its prior position to keep tangent to the inball. We stop, when $y = e^2$ (see Figure 21.2) or L_3 contains the segment $[q^1, q^2]$ (whichever comes first – the first meaning that we arrive in a sailing boat, the latter that we arrive at a triangle).

Before and after the transformation the inradius and the angles in the points y of the two triangles coincide (see Proposition 1.3), while the line passing through the incenter c and y becomes closer to be perpendicular to L_3 . Hence the distance $\text{dist}(y, L_3)$ does not decrease under this movement.

If $y = e^2$, then $C = \text{SB}_{r(K), \gamma(D(K))}$, otherwise, if L_3 contains the segment $[q^1, q^2]$, $C = \text{T}_{r(K), D(K)}$. In both cases $r(C) = r(K), D(C) = D(K), R(C) = R(K)$, and $w(C) = \text{dist}(y, L_3) \geq b_{u^3}(K) \geq w(K)$ holds.

- (v) If $y \in \text{int}(\mathbb{B})$, we rotate the lines L_1, L_2 around q^1, q^2 , respectively, s. t. $y = L_1 \cap L_2$ moves along $\text{aff}\{y, c\}$ away from c . The inball moves, s. t. it remains tangent to L_1 and



21.1: In (iii) the set rotates until $[q^1, q^2]$ becomes parallel to L_3 .

21.2: In (iv) (if $y \in \mathbb{S}$) y moves inside \mathbb{S} and may become e^2 whereas $C = \text{SB}_{r,\gamma}$.

FIGURE 21. Examples of (iii) and (iv) from Lemma 5.5.

L_2 , and L_3 is shifted upwards, parallel to its original position to remain tangent to the inball.

The change finishes when $y \in \mathbb{S}$ or the line L_3 contains the segment $[q^1, q^2]$.

Before and after the movement the triangle T has the same inradius and $\text{aff}\{y, c\}$ has the same angle with respect to L_3 , but the angle in y decreases. Hence the distance $\text{dist}(y, L_3)$ does not decrease.

If we arrive in $y \in \mathbb{S}$, we are in a situation to apply (iv) again. If L_3 contains the segment $[q^1, q^2]$, then we may roll the inball along L_3 and rotate L_i , $i = 1, 2$, s. t. they keep supporting the inball, until $y \in \mathbb{S}$. Hence the inball of $\text{conv}\{y, q^1, q^2\}$ stays equal and it can easily be checked that the width of the triangle does not decrease under this change. In fact, we again arrive in the situation $C = \text{T}_{r(K), D(K)}$ as after (iv), when $y \neq e^2$.

□

Proof of Theorem 3.4. The part of Theorem 3.4 that all sailing boats fulfill equality for (ub_2) directly follows from Lemma 5.5. Thus it only remains to show the general validity of the inequality (ub_2) .

Since there exist isosceles triangles I_γ and concentric sailing boats $\text{SB}_\gamma^\circledast$ of the same diameter and circumradius as a given K for an appropriate choice of $\gamma \in [\pi/3, \pi/2]$, we only have to distinguish the cases

$$(i) \quad r(K) \leq r(I_\gamma), \quad (ii) \quad r(I_\gamma) \leq r(K) \leq r(\text{SB}_\gamma^\circledast), \quad (iii) \quad r(K) \geq r(\text{SB}_\gamma^\circledast).$$

Again we abbreviate $r = r(K)$, $w = w(K)$, $D = D(K)$, and $R = R(K) = 1$.

In case of (ii), K fulfills the conditions of Lemma 5.5 and we obtain $w \leq w(\text{SB}_{r,D})$, which suffices as mentioned above. For the other two cases we *extend* the construction of the general sailing boats from Subsection 4.3:

For any pair r, D obtained from K , let $I_\gamma = \text{conv}\{p^1, p^2, p^3\}$, $\gamma \in [\pi/3, \pi/2]$ be the isosceles triangle with circumball \mathbb{B} and diameter $D = \|p^1 - p^2\|$ as well as $I_K := r/r(I_\gamma)(I_\gamma - p^3) + p^3$ the rescaled copy with inradius r , keeping the vertex p^3 .

By construction, I_K belongs to the general sailing boats, $D(I_K) = r/r(I_\gamma)D$, and $R(I_K) = r/r(I_\gamma)R$. Hence it fulfills (ub_2) with equality. However, since

$$r(I_K) \left(1 + \frac{2\sqrt{2}R(I_K)}{D(I_K)} \sqrt{1 + \sqrt{1 - \left(\frac{D(I_K)}{2R(I_K)}\right)^2}} \right) = r \left(1 + \frac{2\sqrt{2}R}{D} \sqrt{1 + \sqrt{1 - \left(\frac{D}{2R}\right)^2}} \right)$$

it suffices to show that $w \leq w(I_K)$.

Now, we first consider case (i).

Using Lemma 5.5 and the notation used there, we know there exists a triangle $T_{r,D} = \text{conv}\{q^1, q^2, y\}$ in the triangle face, s. t. $\|q^1 - q^2\| = D$ and $w \leq w(T_{r,D}) = \text{dist}(y, [q^1, q^2])$. Hence we just need to prove $w(T_{r,D}) \leq w(I_K)$.

Similar to (iv) of Lemma 5.5, we now transform $T_{r,D}$ by moving y within \mathbb{S} until $y = p^3$, ignoring the stopping condition “when L_3 contains $[q^1, q^2]$ ”. Because of ignoring the stopping condition, the inball will not touch $[q^1, q^2]$ anymore, but a line L parallel to $[q^1, q^2]$, which means that we arrived at a triangle congruente with I_γ and inradius r , which is I_K . Thus $\text{dist}(p^3, L) = w(I_K)$ and we may argue as in (iv) of Lemma 5.5 that $w(T_{r,D}) \leq w(I_K)$, which shows the assertion.

Finally, assume we are in case of (iii). We know from Subsection 4.3 that the outer parallel bodies K' of a concentric sailing boat or a Reuleaux blossom satisfy $r(K') = r$, $D(K') = D$, $R(K') = R$, and $w \leq w(K') = r(K') + R(K')$. Hence we just need to show that $w(K') \leq w(I_K)$ again.

Now, consider the concentric sailing boat SB_γ° . It shares p^3 and its inside angle γ with I_K and has a smaller inradius. Thus it follows from the concentricity of the in- and circumradius of SB_γ° that $c_2 < 0$ holds for the incenter c of I_K has a negative second component η . Hence $w(I_K) = r + R + |c_2| \geq r(K') + R(K') = w(K')$ which finishes the proof. \square

Proof of Theorem 3.6. In case of $r(K) \leq r(I_{\arcsin(D(K)/2R(K)})$) Part (a) of Lemma 5.5 implies $w(K) \leq w(T_{r,D})$, proving the validity of (ub_3) in that case.

Thus we may assume w. l. o. g. that $r(K) \geq r(I_{\arcsin(D(K)/2R(K)})$). Observe two facts: first, if $r(K) = r(I_{\arcsin(D(K)/2R(K)})$, then the two right hand sides of (ub_2) and (ub_3) coincide and equal $w(I_{\arcsin(D(K)/2R(K)})$. Omitting again the argument K , we obtain

$$(8) \quad \frac{w}{r} = 1 + \frac{2\sqrt{2}R}{D} \sqrt{1 + \sqrt{1 - \left(\frac{D}{2R}\right)^2}} = \frac{2}{D} \left(D + \frac{2rR}{D} \left(1 + \sqrt{1 - \left(\frac{D}{2R}\right)^2} \right) \right)$$

in that case. The second fact to be observed is that in (8) the middle expression does not depend on r , while the right hand part is increasing in r . Hence knowing the general validity of (ub_2) , we may conclude

$$\frac{w}{r} \leq 1 + \frac{2\sqrt{2}R}{D} \sqrt{1 + \sqrt{1 - \left(\frac{D}{2R}\right)^2}} \leq \frac{2}{D} \left(D + \frac{2rR}{D} \left(1 + \sqrt{1 - \left(\frac{D}{2R}\right)^2} \right) \right).$$

\square

Now, we turn to the open part of the lower boundary and start with a technical corollary needed in order to prove Theorem 3.2.

Corollary 5.6. *Let $K \in \mathcal{K}^n$ and $c \in \mathbb{R}^n$, s. t. $c + r(K)\mathbb{B}$ and \mathbb{B} are the in- and circumball of K , respectively, $p^1, \dots, p^k \in K \cap \mathbb{S}$ be the points given by Part (a) of Proposition 1.2, $T' := \text{conv}\{p^1, \dots, p^k\}$, and $C := \text{conv}(T', c + r(K)\mathbb{B})$. Then $D(C) = \max\{D(T'), \|p^i - c\| + r(C), i \in [k]\}$.*

Proof. Since the statement is obviously true if $K = \mathbb{B}$, we may assume w. l. o. g. that $K \neq \mathbb{B}$ and therefore $C \neq \mathbb{B}$. This means the diameter of C is bigger than $2r(C)$, the distance of two antipodal points of the inball, but due to Proposition 1.1 attained between two extreme points.

Thus if it is not attained between a pair of the vertices p^1, \dots, p^k , it must be between one of them and its antipodal on the insphere. \square

Remark 5.7. *Let $K \in \mathcal{K}^2$, $c \in \mathbb{R}^2$, $p^1, \dots, p^k \in K \cap \mathbb{S}$, T' , and C be given as in Corollary 5.6. Denoting by L_1, L_2 a pair of parallel supporting lines of C , s. t. $w(C) = d(L_1, L_2)$ we may assume w. l. o. g. due to Proposition 1.1 that L_1 has at least two contact points with C and (by renaming and defining $p^3 = p^2$ if necessary) that p^1 is situated in one of the arcs in \mathbb{S} between L_1 and L_2 , while p^2 and p^3 belong to the other with p^2 closer to L_1 and p^3 closer to L_2 . With this assumptions one of the following cases holds:*

- (i) L_1 contains p^2 but not p^1 and supports $c + r(K)\mathbb{B}$, whereas L_2 supports $c + r(K)\mathbb{B}$.
- (ii) L_1 contains p^2 but not p^1 and supports $c + r(K)\mathbb{B}$, whereas L_2 contains only p^3 .
- (iii) L_1 contains p^1 but not p^2 and supports $c + r(K)\mathbb{B}$, whereas L_2 contains only p^3 .
- (iv) L_1 contains $[p^1, p^2]$, whereas L_2 contains p^3 or supports $c + r(K)\mathbb{B}$.

Due to Proposition 1.1 one of the sets $L_i \cap C$, $i = 1, 2$, say $L_1 \cap C$ contains a smooth boundary point of C . Hence $L_1 \cap C$ is either a segment containing at least one of the points p^1, p^2 , which means we are in Case (ii), (iii), or (iv), or L_1 supports the inball in a unique point (see Figure 22.1 for an example of Case (ii)). However, in case $L_2 \cap C$ is a segment, we may interchange the roles of L_1 and L_2 arriving again in Case (ii), (iii), or (iv), or if L_2 also supports C only in a single boundary point of the inball, we may rotate L_1 and L_2 around it, s. t. we may assume Case (i).

The following lemma proves Theorem 3.2 apart from the general validity of the inequality.

Lemma 5.8. *Let $K \in \mathcal{K}^2$ be s. t. there exists a bent pentagon $\text{BP}_{r,\gamma}$ from the facet (lb_3) with the same inradius, circumradius, and diameter as K . Then $w(K) \geq w(\text{BP}_{r,\gamma})$.*

Proof. Using the same notation as in Corollary 5.6 we have $r(C) = r(K)$ and $R(C) = R(K)$ by definition as well as $D(C) \leq D(K)$ and $w(C) \leq w(K)$ because of the monotonicity of the radii with respect to set inclusion.

The idea of the proof is to transform C in several steps into a bent isosceles $\text{BI}_{r,\gamma}$ from (lb_3) of Subsection 4.3 keeping the same in- and circumradius at all time and guaranteeing that $D(\text{BI}_{r,\gamma}) = D(K)$ and $w(\text{BI}_{r,\gamma}) \leq w(K)$ at the end of the transformation (and obtaining the corresponding solution for $\text{BP}_{r,\gamma}$). More precisely, we know that the parallel supporting lines L_1 and L_2 of C from Remark 5.7 satisfy $w(C) = d(L_1, L_2)$. Now, in every step of the transformation of C , $d(L_1, L_2)$ will be decreased, however when arriving at $\text{BI}_{r,\gamma}$ it again holds $w(\text{BI}_{r,\gamma}) = d(L_1, L_2)$ (as shown in (lb_3)).

To reduce notation formalities we assume w. l. o. g. that L_1, L_2 are embedded horizontally and we denote the inball by $c + r\mathbb{B}$.

- (a) The first step is only needed in case of $c_1 < 0$. In this step all radii except the diameter of C are kept constant, while the diameter may be reduced but not raised.

If L_1 and L_2 are arranged as in Case (iii) of Remark 5.7, then using Part (b) of Proposition 1.1, we see that $c_1 < 0$ is not possible as $c_1 \geq p_1^3 \geq 0$ holds. In case of (ii) or (iv), we may translate B parallel to L_1 until $c_1 = 0$. Because of Corollary 5.6 this

transformation does not increase $D(C)$: in both cases the only candidate distance for the diameter which is raised is $\|p^1 - c\| + r(C)$, but in case of (iv) $\|p^1 - c\|$ is before and after the transformation bounded from above by $\|p^2 - c\|$ and in case of (ii) it is bounded from above by $\|p^2 - c\|$ or by $\|p^3 - c\|$.

Finally, Case (i) can be handled almost the same. If p^3 is closer to L_2 than p^1 , again $\|p^2 - c\|$ is bounded from above by $\|p^2 - c\|$ or by $\|p^3 - c\|$ and we may directly move B parallel to L_1 until $c_1 = 0$. If, on the contrary, p^1 is the point closer to L_2 , then we first rotate C between L_1 and L_2 until p^1 and p^3 get into same distance to L_2 and then we may do the movement of B .

- (b) Translate p^2 and p^3 on \mathbb{S} within the arcs between L_1 and L_2 they belong to, until $\|p^1 - p^2\| = \|p^1 - p^3\| = D(K)$. Since $c_1 \geq 0$ and $D(C) \leq D(K)$ before the transformation we have $D(C) = D(K)$ after the transformation and we keep at least p^1 on L_1 or L_1 tangent to the unit ball. Moreover, if necessary, moving L_2 parallel to its prior position until it supports C again, L_2 touches p^3 or $c + r\mathbb{B}$ (see Figure 22.1), $d(L_1, L_2)$ does not increase, and $r(C)$ and $R(C)$ stay constant.

However, in each situation where we only touch two points after the transformation, we may additionally rotate L_1 and L_2 around the vertices or along the insphere, respectively, not increasing their distance, until we obtain a third touching point of the two lines with C . In the following we distinguish the following cases, (exchanging, if necessary, the roles of L_1, L_2 and p^2, p^3 , respectively, to attain one of them)

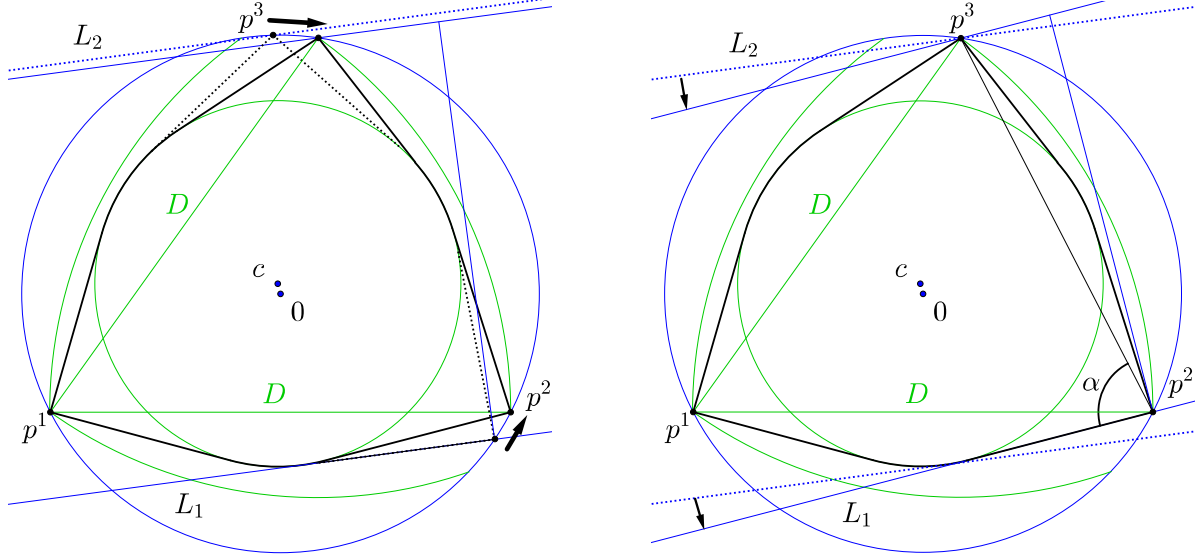
- (i) L_1 contains p^1 , or
- (ii) L_1 contains p^2 and supports $c + r\mathbb{B}$ and L_2 contains p^3 , or
- (iii) L_1 does not contain any of the points p^i , while L_2 contains p^3 but no other.

In all three cases we will search for a situation, in which the angle between L_1 with one of the edges of I_γ is acute. If (i) holds, the angle between L_1 and $[p^1, p^3]$ must always be acute as p^3 lies on the right side of p^1 .

In case of (ii), the angle between L_1 and $[p^2, p^3]$ can either be acute (see Figure 22.2) or obtuse, as p^3 could even be on the right of p^2 . If the latter happens we rotate L_1 around p^2 (thus possibly loosing contact with $c + r\mathbb{B}$) and L_2 around p_3 , keeping them parallel, until L_2 supports $c + r\mathbb{B}$, allowing a zero degree rotation in the case that L_2 supported $c + r\mathbb{B}$ from the beginning. This does not increase $d(L_1, L_2)$.

Finally if (iii) holds, the angle between L_2 and $[p^2, p^3]$ could be obtuse. Then we rotate both lines L_1, L_2 along $c + r\mathbb{B}$, loosing contact with p^3 , until L_2 touches p^1 or L_1 touches p^2 (whichever comes first). In case L_2 touches p^1 first we are back in (i). Thus assume L_1 touches p^2 first. Compare with the bent isosceles $\text{BI}_{r,\gamma}$ we want to arrive at: Because of our movement in the beginning of (b), we have that $\text{conv}\{p^1, p^2, p^3\}$ is an isosceles triangle with inball $c + r\mathbb{B}$ contained in C . Thus identifying it with $I_\gamma \subset \text{BI}_{r,\gamma}$ yields that the supporting lines L'_1, L'_2 of $\text{BI}_{r,\gamma}$ contain p^2 and p^3 , respectively, and contain between them the inball of radius r . Thus it holds $\|p^2 - p^3\| \geq 2r$. Considering C again, since the angle between L_2 and $[p^2, p^3]$ was obtuse before the rotation of L_1, L_2 in (iii), the incenter c is closer to p^3 than to p^2 . But since $\|p^2 - p^3\| \geq 2r$, this means after the rotation the angle between L_1 and $[p^2, p^3]$ must be acute. Exchanging if necessary L_1 with L_2 and p^2 with p^3 , we are back again in the cases (i), (ii), (iii) or (iv) of Remark 5.7, also not guaranteeing that the distance between those lines defines the width of C , but knowing that the angle between L_1 and $[p^2, p^3]$ (if (i), (ii) or (iv) hold) or L_1 and $[p^1, p^3]$ (if (iii) holds) is acute (see Figure 23).

- (c) In the last step of the transformation of C we only move $c + r\mathbb{B}$ and L_1, L_2 , keeping $r(C), D(C)$, and $R(C)$ constant. Independently of the tangencies (i)–(iv) of Remark 5.7, $c + r\mathbb{B}$ is translated until it becomes tangent with the pair of arcs with centers p^1, p^2



22.1: In (b), the tangencies correspond to Part (ii) of Remark 5.7. While moving p^2, p^3, L_1 and L_2 some of the tangencies can be lost but we obtain that I_γ is contained in C .

22.2: We rotate L_1, L_2 around C until L_1 or L_2 supports more than one point of C , arriving, e. g., in the situation in which L_1 contains p^2 and supports $c + r\mathbb{B}$, L_2 supports p^3 , and α is acute here. Then we are back into the tangencies of Part (ii).

FIGURE 22. Transformations of C during (b). Here the green bows indicate arcs of radius D and centers in p^1, p^2, p^3 , defining a region in which both, $c + r\mathbb{B}$ and the p^i , have to be contained.

and radius $D(K)$, finishing the transformation of C into $\text{BI}_{r,\gamma}$. Finally L_1 is rotated around p^1 (in case of Part (iii) of Remark 5.7) or around p^2 (in all other cases) keeping it tangent to $c + r\mathbb{B}$ and L_2 keeping it parallel to L_1 and supporting C . A simple but crucial observation is the following: assuming that L_1 contains p^2 , it was shown in (lb₃) of Subsection 4.3 that $c + r\mathbb{B}$ is the inball of $\text{BP}_{r,\gamma}$, touching its boundary in the diametrical arcs around p^1, p^2 and in L_1 . Therefore any translation of $c + r\mathbb{B}$ within the region spanned by the two arcs would lead to an intersection of L_1 with the interior of $c + r\mathbb{B}$, which means that before the rotation of L_1 , its angle with $[p^2, p^3]$ was not smaller than after. This observation implies that the breadth $b_s([p^2, p^3])$ with s orthogonal to the two lines is reduced by the rotation.

However, in Cases (ii) and (iii) of Remark 5.7 it obviously holds $b_s([p^2, p^3]) = d(L_1, L_2)$ and since $d(L_1, L_2)$ did not increase in any step of the transformation we obtain $w(K) \geq d(L_1, L_2) \geq w(C)$.

Finally, consider the remaining cases, (i) and (iv): they describe the extremal situation when C shares radii with a set from the edges (BT, H) or (BT, FR) . In case of (i) L_1 and L_2 support $c + r\mathbb{B}$, which means $d(L_1, L_2) = 2r$ and therefore that $w(C) = d(L_1, L_2) \leq w(K)$. In case of (iv) we have $L_1 \supset [p^1, p^2]$ and $p^3 \in L_2$ parallel to L_1 . Hence $w(C) \leq d(L_1, L_2) = w(I_\gamma)$, within the given parameters for γ , and since $I_\gamma \subset C$ it follows $w(C) = d(L_1, L_2)$.

□

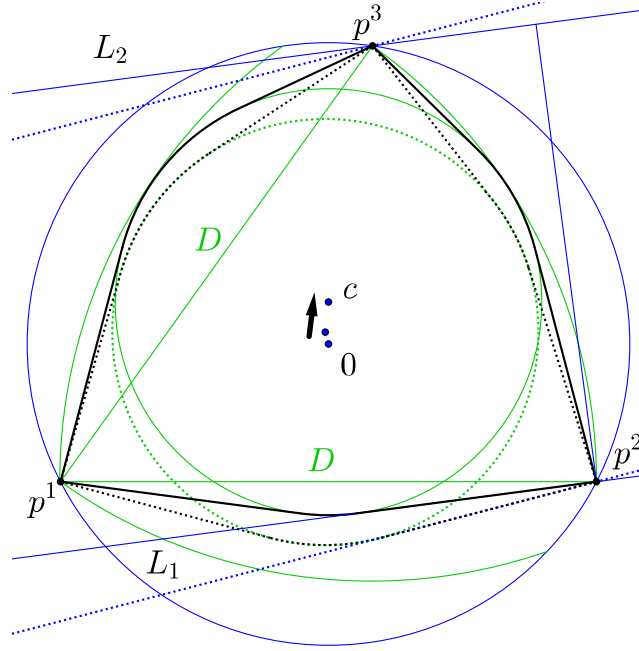


FIGURE 23. In (c) the inball moves, L_1 is rotated around p^2 reducing the angle with $[p^2, p^3]$ and L_2 to keep parallel with L_1 until $C = \text{BI}_{r,\gamma}$.

Proof of Theorem 3.2. As before we abbreviate $r(K) = r$ and the same for the other radii. In order to show the general validity of the inequality (lb_3) , we split the proof into the following cases:

- (i) $8r \geq 3D, \gamma \geq \gamma_r, r \leq r(\mathbb{H}),$ (ii) $8r < 3D$
- (iii) $\gamma < \gamma_r, r(\mathbb{BT}) \leq r \leq r(\mathbb{H}),$ (iv) $r > r(\mathbb{H}).$

Recognize that in case of (i) there exists a bent pentagon $\text{BP}_{r,\gamma}$, as we have shown with the help of Lemma 4.2 in (lb_3) . Thus we are under the conditions of Lemma 5.8 in that case.

In the remaining cases, consider the generalized bent pentagon $\text{BP}_{r,\gamma}$ as defined in the description of the facet (lb_3) (together with all the notation used there) and observe that the distance $d(L_1, L_2)$ may in any case be computed as the width in (7). The angle β may become $-\beta$ in Case (ii) (cf. Figure 24) or the angle μ may become $-\mu$ in Cases (iii) or (iv), whenever the angle between L_1 and $[p^2, p^3]$ is bigger than $\pi/2$. In both cases this change of sign does not affect the final value of the right hand side of the inequality (lb_3) to coincide with $d(L_1, L_2)$.

Hence it suffices to show $w \geq d(L_1, L_2)$. For this assume w. l. o. g. that $[p^1, p^2]$ is horizontal and below 0, that $p_1^1 \leq p_1^2$, and that $p_2^3 \geq 0$.

In case of (ii), Part (a) of Lemma 4.2 ensures that $[p^1, p^2]$ does not intersect $c + r\mathbb{B}$. Thus the slope of the L_i 's is negative, and considering the line L containing $[p^1, p^2]$, the angle between L_1 and $[p^2, p^3]$ is smaller than the angle between L and $[p^2, p^3]$ (cf. Figure 24). Hence, denoting the line containing p^3 and parallel to L by L' , their distance satisfies $d(L_1, L_2) \leq d(L, L') = w(\text{I}_\gamma) \leq w$.

Now, let us assume that (iii) is true, but not (ii). Then we know from Part (b) of Lemma 4.2, that the distance $d(L_1, L_2)$ decreases if γ decreases. Using $\gamma \leq \gamma' = \gamma_r$ we obtain $d(L_1, L_2) \leq d(L'_1, L'_2) = w(\text{BI}_{r,\gamma_r}) = 2r \leq w$.

Finally, for the treatment of (iv), one should first observe two easy facts: first, since $p^2 \in L_1$ and $p^3 \in L_2$ we have $d(L_1, L_2) \leq \|p^2 - p^3\|$ and second if $r = r(\mathbb{H}), \gamma = 2 \arccos(D(\mathbb{H})/2)$, and

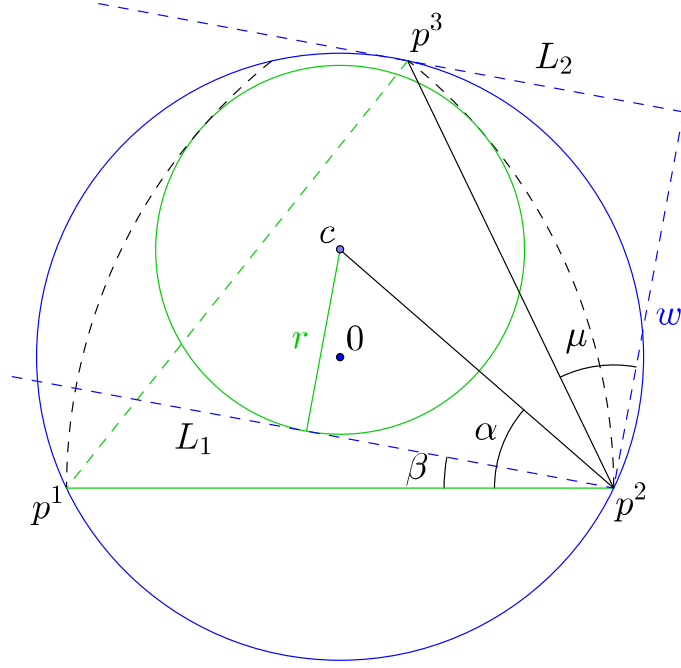


FIGURE 24. If $3D > 8r$, the angle β in the computations in lb_3 (cf. Figure 15.1) becomes $-\beta$, but does not change the final equation for $d(L_1, L_2)$.

$L_1^{\mathbb{H}}, L_2^{\mathbb{H}}$ are the according support lines of \mathbb{H} , then $L_1^{\mathbb{H}}, L_2^{\mathbb{H}}$ are perpendicular to $[p^2, p^3]$ and thus $\|p^2 - p^3\| = w(\mathbb{H}) = 2r(\mathbb{H})$ (cf. the description of \mathbb{H} in Subsection 4.1). From (iv) and inequality (ib₂) we obtain that $D(\mathbb{H}) = r(\mathbb{H}) + 1 \leq r + 1 \leq D$ and since $[p^2, p^3]$ is the shorter edge of L_γ we have $\|p^2 - p^3\| = D/R \sqrt{4R^2 - D^2}$ which is a decreasing function on D . Hence $\|p^2 - p^3\|$ is maximized, when $\gamma = \gamma_r$, i. e. when $\|p^2 - p^3\| = w(\mathbb{H})$. Thus using inequality (lb₁) we obtain

$$d(L_1, L_2) \leq \|p^2 - p^3\| \leq w(\mathbb{H}) = 2r(\mathbb{H}) \leq 2r \leq w,$$

which completes the proof. \square

6. FINAL REMARKS

For finishing the paper, let us give two final remarks:

First, for some practical purposes it could be of some value to be able to replace the sometimes quite unhandy non-linear inequalities by linear ones. Thus knowing the full extend of the diagram know, it would be worthwhile to develop a complete system of linear inequalities supporting the diagram. Since the convex hull of the vertices does not contain the full diagram (the supporting plane of $\mathbb{L}, \mathbb{I}_{\pi/3}$, and $\mathbb{I}_{\pi/2}$ separates $\text{SB}_\gamma^\circledast$ from major parts of the diagram) and since all edges and facets are smooth, this system cannot be finite.

Second, especially considering the application of Blaschke-Santaló diagrams given in [8, 7, 15], consider the following problem: suppose two convex sets K and K' are mapped to the same point in the diagram, how “different” may K and K' be? Before giving any answer to this question, we should first develop an idea, how to measure this “difference”. For this neither the usual Hausdorff nor the Banach-Mazur distance can be taken. For the Hausdorff distance any K and some of its rotations may be quite far from each other, while the Banach-Mazur distance would mark (e. g.) all simplices equal. A good choice for this task could be taking

the Hausdorff distance within the class of similarities of the two sets. However, to the best of our knowledge, this distance is not considered in literature so far.

Acknowledgements: We would like to thank Viviana Ghiglione and Evgeny Zavalnyuk for giving crucial hints, as well as Peter Gritzmann, Maria Hernández Cifre, and Salvador Segura Gomis for always supporting us.

REFERENCES

- [1] W. Blaschke, Eine Frage Über Konvexe Körper, *Jahresber. Deutsch. Math. Ver.*, **25** (1916), 121-125.
- [2] T. Bonnesen, W. Fenchel, *Theorie der konvexen Körper*. Springer, Berlin, 1934, 1974. English translation: *Theory of convex bodies*. Edited by L. Boron, C. Christenson and B. Smith. BCS Associates, Moscow, ID, 1987.
- [3] K. Böröczky Jr., M. A. Hernández Cifre and G. Salinas, Optimizing area and perimeter of convex sets for fixed circumradius and inradius, *Monatsh. Math.* **138** (2003), 95–110.
- [4] R. Brandenburg, Radii of convex bodies, Ph.D. thesis, Zentrum Mathematik, Technische Universität München, 2002.
- [5] R. Brandenburg, S. König, No dimension-independent core-sets for containment under homothetics, *Discrete Comput. Geom.* **49** (1) (2013), 3–21.
- [6] R. Brandenburg, S. König, Sharpening geometric inequalities using computable symmetry measures, arXiv:1310.4368.
- [7] J. Debayle, J. C. Pinoli and B. Presles, Shape recognition from shadows of 3-D convex geometrical objects, *19th IEEE International Conference on Image Processing (ICIP)*, 2012, 509–512.
- [8] J. Debayle, S. Rivollier and J. C. Pinoli, Adaptive Shape Diagrams for Multiscale Morphometrical Image Analysis, *J. Math. Imaging Vis.* 2013.
- [9] P. Gritzmann, V. Klee, Inner and outer j -radii of convex bodies in finite-dimensional normed spaces, *Discrete Comput. Geom.* **7** (1992), 255–280.
- [10] M. A. Hernández Cifre, Is there a planar convex set with given width, diameter and inradius?, *Amer. Math. Monthly*, **107** (2000), 893–900.
- [11] M. A. Hernández Cifre, Optimizing the perimeter and the area of convex sets with fixed diameter and circumradius, *Arch. Math.* **79** (2002), 147–157.
- [12] M. A. Hernández Cifre, E. Saorín, On the roots of the Steiner polynomial of a 3-dimensional convex body, *Adv. Geom.*, **7** (2007), 275–294.
- [13] M. A. Hernández Cifre, S. Segura Gomis, The missing boundaries of the Santaló diagrams for the cases (d, w, R) and (w, R, r) , *Discrete Comp. Geom.*, **23** (2000), 381–388.
- [14] H. Jung, Über die kleinste Kugel, die eine räumliche Figur einschließt, *J. Reine Angew. Math.* **123** (1901), 241–257.
- [15] B. Presles, Caractérisation géométrique et morphométrique 3D para analyse d’images 2D de distributions dynamiques de particules convexes anisotropes, Ph. D. Thesis, 2011.
- [16] J. R. Sangwine-Yager, The missing boundary of the Blaschke diagram, *Amer. Math. Monthly*, **96** (1989), 233-237.
- [17] L. Santaló, Sobre los sistemas completos de desigualdades entre tres elementos de una figura convexa planas, *Math. Notae*, **17** (1961), 82–104.
- [18] R. Schneider, Convex Bodies: The Brunn-Minkowski Theory, *Cambridge University Press*, Cambridge, 1993.
- [19] P. R. Scott, Sets of constant width and inequalities, *Quart. J. Math. Oxford Ser.*, **32** (1981), 345–348.
- [20] P. Steinhagen, Über die größte Kugel in einer konvexen Punktmenge, *Abh. Hamb. Sem. Hamburg*, **1** (1921), 15–26.
- [21] L. Ting and J. B. Keller, Extremal convex planar sets, *Discrete Comput. Geom.* **33** (2005), no. 3, 369–393.

ZENTRUM MATHEMATIK, TECHNISCHE UNIVERSITÄT MÜNCHEN, BOLTZMANNSTR. 3, 85747 GARCHING BEI MÜNCHEN, GERMANY
E-mail address: brandenb@ma.tum.de

DEPARTAMENTO DE MATEMÁTICAS, UNIVERSIDAD DE MURCIA, CAMPUS ESPINARDO, 30100-MURCIA, SPAIN
E-mail address: bgmerino@um.es